Functional role of α-actinin, PI 3-kinase and MEK1/2 in insulin-like growth factor I receptor kinase regulated motility of human breast carcinoma cells

Marina A. Guvakova[1,*], Josephine C. Adams[2,3] and David Boettiger[1]

[1]Department of Microbiology, University of Pennsylvania, 3610 Hamilton Walk, 211 Johnson Pavilion, Philadelphia PA 19104, USA
[2]MRC-Laboratory for Molecular Cell Biology and Department of Biochemistry and Molecular Biology, University College London, Gower Street, London WC1E 6BT, UK
[3]Department of Cell Biology, Building NC1, Lerner Research Institute, Cleveland Clinic Foundation, 9500 Euclid Avenue, Cleveland, Ohio 44195, USA
*Author for correspondence (e-mail: guvakova@mail.med.upenn.edu)

Accepted 19 August 2002
Journal of Cell Science 115, 4149-4165 © 2002 The Company of Biologists Ltd
doi:10.1242/jcs.00104

Summary

Within epithelial tissue, cells are held together by specialized lateral junctions. At particular stages of development and in pathological processes such as metastasis, cells break down the intercellular junctions, separate from the epithelial sheet and migrate individually. Despite the importance of these processes, little is understood about the regulatory mechanisms of active cell separation. In view of the effects of insulin-like growth factor I (IGF-I) on mammary gland development and cancer, we developed a model using MCF-7 human breast cancer cells in which the process of cell separation can be induced by IGF-I. The separation was enhanced in MCF-7 cells overexpressing the IGF-IR and blocked in the cells expressing a dead-kinase mutant of this receptor. Activation of the IGF-IR resulted in a rapid formation of motile actin microspikes at the regions of cell-cell contacts, disorganization of mature adherens junctions and the onset of cell migration. In cell separation, the signaling between the IGF-IR kinase and actin required phosphatidylinositol 3 (PI 3)-kinase-generated phospholipids but not MAP kinases and was mediated by α-actinin. The activity of MEK1/2 kinases was needed for consecutive cell migration. This work also defined a new function for α-actinin. Upon IGF-IR activation, green fluorescence protein (GFP)-labeled α-actinin concentrated at the base of actin microspikes. Deletion of the N-terminal actin-binding domain of α-actinin prevented this redistribution, indicating that this domain is necessary. Deletion of the C-terminal tail of α-actinin reduced the number of microspikes, showing that α-actinin has a role in the development of microspikes and is not passively reorganized with filamentous actin. We suggest that the signaling pathway from the IGF-IR kinase through the PI-3 kinase to α-actinin participates in the rapid organization of actin into microspikes at the cell-cell junctions and leads to active cell separation, whereas signaling through ERK1/2 MAP kinases controls cell migration following cell separation.

Movies available on-line

Key words: IGF-IR signaling, α-actinin, Actin cytoskeleton, Breast cancer cell migration

Introduction

Differentiated epithelial cells are organized in contiguous layers that protect the underlying connective tissue from the external environment and comprise the parenchyma of the inner organs such as the glands. The lateral membranes of these adherent cells are connected via highly specialized adhesive junctions whose formation and maintenance is critically dependent on linkage to the cytoskeleton: tight and adherens junctions are linked to the cortical actin, whereas desmosomes are connected to the network of intermediate filaments (Cowin and Burke, 1996; Davies and Garrod, 1997). This unique tissue architecture allows epithelial cells to remain relatively static, except for during cell separation and migration that occur in development, tissue regeneration and metastasis (Gumbiner, 1996).

Some mechanistic aspects and common sequential changes that precede cell separation have been determined using animal and cellular models (reviewed in Hay, 1995; Thiery and Chopin, 1999; Savagner, 2001). For example, epithelial colonies can be induced to separate by treatment with physiological peptides, including hepatocyte growth factor/scatter factor (HGF/SF), neuregulin, members of the fibroblast growth factor (FGF), epidermal growth factor (EGF) and transforming growth factor (TGF) families (Stoker and Perryman, 1985; Savagner et al., 1997; Chausovsky et al., 1998; Müller et al., 1999). Peptides with cell scattering function induce a disruption of intercellular junctions, a reorganization of the actin cytoskeleton and an increase in local cell motility. These effects are mediated by receptor tyrosine kinases (Sachs et al., 1996), of which the most extensively studied is Met, the receptor for HGF/SF (reviewed in Furge et al., 2000). Activation of Met has a

strong effect on scattering and invasiveness of the rodent mammary epithelial cells and various human carcinoma cell lines, and similar disorganization is believed to lead to metastasis (Wiedner et al., 1990; Liang et al., 1996; Firon et al., 2000). It is less clear, however, whether HGF/SF and Met control motile behavior of human breast tumor cells. No scattering response to HGF/SF has been seen in human breast carcinoma cell lines in vitro (Stoker et al., 1987); in breast tissue biopsies, the intensity of Met staining was lower in tumor tissue than in normal cells adjacent to mammary ducts (Tsarfaty et al., 1992).

Another member of the receptor tyrosine kinase family is the receptor for IGF-I, a protein of particular interest for the biology of the human mammary gland. There is a general requirement for IGF-I in terminal end bud formation and ductal morphogenesis in the developing gland (Kleinberg et al., 2000). In humans, the IGF-IR is expressed by both normal and tumor mammary cells; yet the level of the receptor expression and its tyrosine kinase activity is higher in malignant compared with benign and normal tissues (Happerfield et al., 1997; Resnik et al., 1998). The signaling mechanisms evoked by IGF-IR kinase are well documented (reviewed by LeRoith, 2000). Ligand-induced activation of the IGF-IR causes the sequential phosphorylation of three conservative tyrosines within the catalytic domain, followed by phosphorylation of the cytoplasmic domain of the receptor, recruitment of adapter molecules and initiation of signaling cascades. The two best-characterized pathways triggered by the activation of this receptor are the PI3-kinase signaling via the insulin receptor substrates (IRSs) and the MAP kinase pathway via adaptor molecules Shc. Although IGF-I may have a pleiotropic effect on cell proliferation, differentiation and migration (Leventhal and Feldman, 1997; Lee et al., 1998; Chernicky et al., 2000), the range of IGF-IR activities is critically dependent on the cell context (Baserga, 1999). There is good evidence that in cultured mammary epithelial cells the IGF-IR stimulates not only proliferative but also motile cell responses (Kohn et al., 1990; Doerr and Jones, 1996; Mira et al., 1999). We have recently reported that IGF-I treatment of breast cancer cells overexpressing IGF-IR results in a disruption of the epithelial sheet, implying a role for this receptor in concomitant reorganization of the actin cytoskeleton and cellular junctions (Guvakova and Surmacz, 1999).

The most prominent epithelial structures relying on the actin cytoskeleton are adherence junctions. The core of these junctions is composed of transmembrane E-cadherins and cytoplasmic α,β- and γ-catenins (reviewed by Gumbiner, 2000). α-catenin directly or via actin-binding proteins α-actinin and vinculin couples cadherin-catenin complexes to microfilaments (Knudsen et al., 1995; Nieset et al., 1997; Vasioukhin et al., 2000). Such a linkage is essential for the stabilization of intercellular adhesion and the maintenance of mammary epithelial tissue (Tsukatani et al., 1997). On the basis of the correlation between upregulation of the IGF-IR in breast tumors and the effects of the overexpressed IGF-IR on the actin cytoskeleton, we hypothesize that high levels of IGF-IR activity can induce destabilization of cell-cell contacts. We report a novel signaling effect of the IGF-IR kinase in coupling α-actinin and actin-containing microspikes by a PI 3-kinase-dependent mechanism at an early stage of epithelial cell separation.

Materials and Methods

Cell culture and reagents

MCF-7 human breast cancer cell line (ATCC, HTB-22) and its derivatives were all grown in Dulbecco's Modified Eagle Medium: Nutrient Mixture F-12 (Ham) 1:1 (D-MEM/F-12) containing 5% calf serum (CS), penicillin and streptomycin at 37°C in 5% CO_2. For overnight serum starvation, MCF-7 cells were incubated in phenol-red- and serum-free D-MEM/F-12 containing 0.5 mg/ml bovine serum albumin (BSA). The derivation of a clonal line of MCF-7 that overexpressed the wild-type human IGF-IR 18-fold has been previously described (Guvakova and Surmacz, 1997). This line is referred as MCF-7/IGF-IR/WT in this study. D-MEM/F-12, phenol-red-free D-MEM/F-12, CS and Geneticin (G418) were purchased from Gibco BRL, Life Technologies. LY 294002, PD 98059 and the Akt inhibitor were from Calbiochem, UO126 from Promega and human recombinant IGF-I from Bachem.

Molecular cloning and cell transfection procedures

MCF-7/IGF-IR/DK kinase-deficient cells were generated using a IGF-IR β subunit with mutations in the activation loop of the catalytic domain (three tyrosine residues, Y1131, Y1135, and Y1136 were substituted by phenylalanines). This DNA was a gift from D. Leroith, NIH (Kato et al., 1994). The mutant IGF-IR cDNA was subcloned from the pBluscript II KS+ vector into the *Eco*RI and *Xba*I sites of the pcDNA3 expression vector (Invitrogen Corp., San Diego, CA) under the control of the CMV promoter. MCF-7 cells expressing the mutant receptor were derived by calcium-phosphate-precipitation-mediated transfection with a plasmid encoding the mutant hIGF-IR followed by selection in 2.5 mg/ml G418. Surface expression of the IGF-IR was confirmed by fluorescence-activated cell sorting (FACS) using a monoclonal antibody against the α subunit of the IGF-IR and a secondary FITC-conjugated goat anti-mouse antibody (Vector). Stable clones expressing approximately 1.0×10^6 IGF-IRs per cell were isolated.

For functional analysis of α-actinin, new DNA constructs encoding the truncated α-actinins with enhanced green fluorescent protein (EGFP) tagged to the C-terminus were generated. A full-length chicken sarcomeric α-actinin (GenBank™ accession number X59247) was obtained from J. Sanger (University of Pennsylvania) (Dabiri et al., 1997). A 230 amino-acid N-terminal truncation, including residues 1-24 in the potential site for regulation of high-affinity binding of α-actinin to actin (Xu et al., 1998) and residues 108-189 in the actin-binding site determined by mutagenesis (Hemmings at al., 1992), was produced by excision of a unique 5′ *Eco*47III-*Eco*RV restriction enzyme fragment, followed by blunt-end religation of the truncated plasmid DNA. In this mutant α-actinin RNA, the authentic methionine start codon is removed, and the translation is initiated at the AUG codon for methionine 231. The deletion of the C-terminal tail of α-actinin was generated by excision of a *Sac*I fragment from the plasmid encoding full-length α-actinin, followed by religation of the fragment into the *Sac*I site of pEGFPN1 vector. The authentic initiating codon is retained in this mutant. The removed region encodes 168 amino acids, including a large part of a vinculin-binding site [residues 713-749 (McGregor et al., 1994)] and both EF-hand Ca^{2+}-binding motifs (Baron et al., 1987). The proper deletions were confirmed by restriction mapping of the N- and C-terminal regions of α-actinin cDNA. The position of the truncated α-actinins in frame with EGFP was verified using the Vector NTI version 3.0 program (InforMax, Inc.).

In transient transfection experiments, 5×10^4 MCF-7/IGF-IR/WT or MCF-7/IGF-IR/DK cells were plated into a 35 mm glass-bottomed culture dish (MatTek Corporation, Ashland, MA). The next day, the cells were transfected with plasmids encoding EGFP-α-actinin constructs or the pEGFP-N1 control vector (Clontech) using Lipofectamine Plus Reagent (Gibco, BRL). After 3 hours, the cells were washed in D-MEM/F-12 and incubated overnight in the

conditioned medium of MCF-7/IGF-IR/WT cells to improve the survival of the transfectants. The living cells were used in experiments 48 hours after transfection, when approximately 40% of cells produced fluorescently labeled protein.

Western blotting and immunoprecipitation

Cells were lysed in buffer containing 50 mM Hepes pH 7.5, 150 mM NaCl, 1.5 mM MgCl, 1 mM EGTA, 10% glycerol, 20 μg/ml aprotinin, 1 mM phenylmethylsulfonyl fluoride, 2 mM Na orthovanadate and either 1% Triton X-100 or 1% SDS. For western blots, 20 μg of total protein was resolved by SDS-polyacrylamide gel electrophoresis (SDS-PAGE) and transferred to Hybond ECL nitrocellulose (Amersham Pharmacia Biotech). In a series of experiments, the blots were probed with antibodies against IGF-IR (rabbit polyclonal anti-IGF-IR β subunit, Santa Cruz, SC); IRS-1 (rabbit polyclonal anti-IRS-1, Upstate Biotechnology Inc., UBI, Lake Placid, NY); α-actinin (mouse IgG clone AT6/172, UBI and goat polyclonal anti-α-actinin antobodies, SC); α-catenin (rabbit polyclonal antibodies, Sigma); GFP (mouse monoclonal antibody, Clontech Laboratories, Inc.); phospho-Akt (rabbit anti-phospho-Akt (Ser 473), rabbit anti-phospho-Akt (Thr 308), New England Biolab, NEB); Akt (rabbit anti-Akt, NEB); phospho MAPK (mouse monoclonal E10, anti-phospho-p44-42 MAPK (Thr 202/Tyr 204), NEB); ERK1/ERK2 (rabbit polyclonal k23 anti-ERK1, SC), and phospho-tyrosine-containing proteins (mouse monoclonal PY-20 anti-phosphotyrosine, SC). For immunoprecipitation of α-actinin, 500 μg of total protein from 1% SDS cellular extracts was incubated with 4 μg of anti-α-actinin monoclonal IgG_1, clone AT6/172 (UBI) and 50 μl anti-mouse IgG-agarose beads (Sigma) in HNTG buffer (20 mM Hepes pH 7.5, 150 mM NaCl, 0.1% Triton X-100, 10% glycerol) overnight at 4°C. The immmunoprecipitated proteins were resolved by SDS-PAGE and blotted with anti-α-actinin and PY 20 antibodies. To visualize primary antibody-bound protein, the secondary antibodies conjugated to horseradish peroxidase (1:10,000 dilution; Calbiochem) and the ECL detection solutions (Amersham Pharmacia, UK) were applied. The chemiluminescent intensity of the bands was digitized using the Image Analyser LAS-1000 plus system and the Image Reader LAS-1000 Lite version 1.0 software (Fuji). When several proteins were to be detected on the same membrane, nitrocellulose was incubated in stripping buffer (100 mM 2-mercaptoethanol, 2% SDS, 62.5 mM Tris-HCl pH 6.7) for 30 minutes at 50°C, then washed three times in washing buffer (100 mM Tris pH 7.5, 1M NaCl, 1% Tween-20), blocked in 5% BSA in PBS and re-probed. The relative activity of the protein kinase B (PKB/Akt) and mitogen-activated protein (MAP) kinases was quantified as the ratio of phosphorylated protein to the corresponding total protein detected on the same blot.

Indirect immunofluorescence microscopy

To visualize filamentous actin (F-actin), cells grown on 22 mm (no. 1) glass coverslips were fixed with 3.7% formaldehyde in PBS for 15 minutes, permeabilized with 0.05% Triton X-100 in PBS for 5 minutes and stained with tetramethylrhodamine B isothiocyanate (TRITC)-phalloidin (1 μg/ml) (Sigma) for 30 minutes. Changes in the intracellular distribution of α-actinin were assessed in formaldehyde-fixed cells using an anti-α-actinin antibody (clone BM-75.2; Sigma) (1:200) followed by fluorescein isothiocyanate (FITC)-conjugated goat anti-mouse antibody (Vector). Distribution of α-catenin was assessed in formaldehyde-fixed cells using an anti-α-catenin antibody (Sigma) (1:200) followed by a Rhodamine-Red-conjugated goat anti-rabbit antibody (Jackson ImmunoReseasrch Laboratories, Inc). Fascin was visualized in methanol-fixed cells using antibody 55k-2 as described previously (Guvakova et al., 2002). The samples were examined under a Nikon Eclipse E600 MRC 1024 confocal laser-scanning (Bio-Rad) microscope with a Plan Apo 60×/1.4 oil objective lens (Nikon). Images were acquired using the Bio-Rad LaserSharp 2000 software run under the OS/2 Warp ConnectTM operating system. Images were collected as stacks of xy optical sections (z-series) taken at different focal planes within the sample.

Transmission electron microscopy

Cells were grown to confluence in regular culture medium on 60 mm tissue culture dishes (Falcon). Following overnight serum starvation, cells were either stimulated with 50 ng/ml IGF-I for 15 minutes or kept in serum-free medium at 37°C until fixing. Cells were fixed in fresh fixative (1% glutaraldehyde, 1% OsO_4 in 0.05M phosphate buffer, pH 6.2) for 45 minutes at 4°C (Tilney and Tilney, 1994), washed three times in water at 4°C to remove phosphate, stained with 1% uranyl acetate overnight in the dark at 4°C, dehydrated in ethanol and 2-hydroxypropyl methacrylate and then embedded in an epon substitute LX-112 (Ladd Research Industries Inc, VT). Sections were cut with a diamond knife and examined with a Philips 200 electron microscope (Philips Scientific, Mahwah, NJ). Photographs were taken of sections mounted on uncoated grids. Images of the scanned photographs were processed as Adobe Photoshop files for the figures presented.

Four-dimensional imaging of EGFP-α-actinin dynamics in live cells

Cells grown in glass-bottomed dishes in D-MEM/F-12 containing 15 mM HEPES buffer were placed within a chamber heated at 37°C mounted on the stage of a Nikon Eclipse TE 300 confocal laser-scanning (Bio-Rad) microscope. Multiple replicate fields of cells were observed over 10 minutes in serum-starved cultures or were followed for 10 minutes in the presence of 50 ng/ml IGF-I. For the IGF-I time course study, four-dimensional (4D) data sets (sequences of z-series collected over time) were acquired using the acquisition function of the LaserSharp 2000 (Bio-Rad) software. Digital confocal images were captured in real time as a z series (z-step=0.5 μm) throughout the thickness of each cell. The 4D series was reconstructed into a 3D projection sequence using the LaserSharp processing function. Single sections were selected for export into Photoshop files for the figures presented.

Time-lapse video microscopy

MCF-7, MCF-7/IGF-IR/WT or MCF-7/IGF-IR/DK cells were plated at low density in DMEM/F-12 in Slideflasks (Nunc, Denmark) and allowed to adhere, spread over and establish cell-cell contacts. Time-lapse video microscopy was carried out in a 37°C environmental chamber using a Zeiss Axiovert 100 microscope linked by a Sony SS-M37OCE CCD camera to a video recorder driven by an EOS BAC 900 animation controller. Recordings were made at a rate of 10 frames per minute over a 60-80 minute period for each sample. Each sample contained between 46 to 102 cells per field, and all conditions were analyzed in three independent experiments. Alterations in cell motility and shape were measured from traces of the video images documenting (a) paths of the cell centroid, which were used to calculate cell velocities as movement over time; (b) the changes in cell outline over time, from which the percentage of cells with edge ruffles was calculated; and (c) the appearance of apical ruffles, which appeared as dynamic phase dark ridges at the nuclear and perinuclear regions of the apical cell membrane. In experiments involving IGF-I treatment, video recording was started within 1 minute of adding the growth factor. A QuickTime movie was generated from video records using the Improvision Openlab software package.

Results

The development of a cell model to study the role of the IGF-IR in motility of human epithelial cells

In the present study, we examined the effects of signaling from

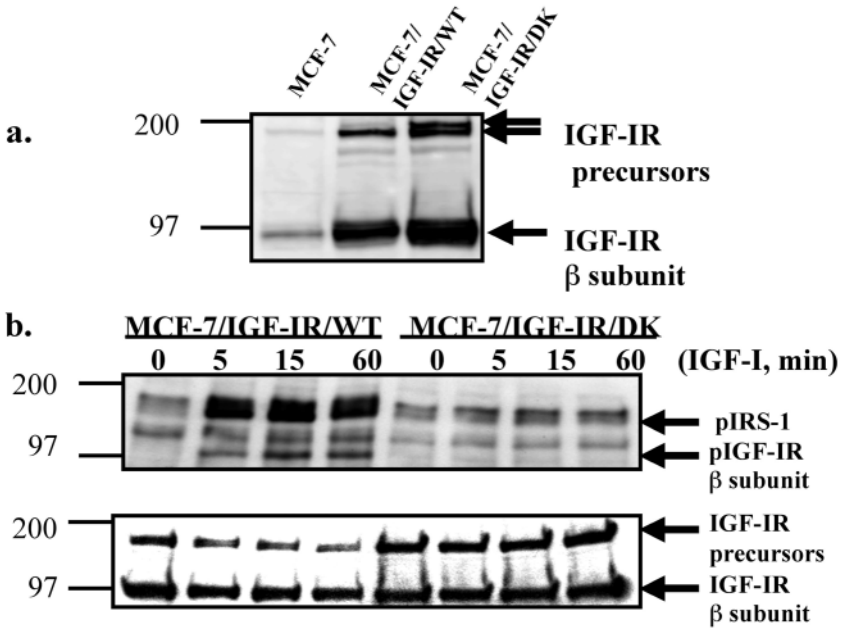

Fig. 1. IGF-IR expression levels and signaling in MCF-7-derived cell lines. (a) Expression of the IGF-IR was detected in MCF-7, MCF-7/IGF-IR/WT and MCF-7/IGF-IR/DK cells by western blotting of 20 μg of total protein with an antibody against the C-terminus of the IGF-IR β subunit. The arrows show the position of the β subunit in the mature receptor (95 kDa) and its precursors: prepro-(190 kDa) and pro-receptor (185 kDa). (b) Top panel: phosphotyrosine blot of MCF-7/IGF-IR/WT and MCF-7/IGF-IR/DK cells stimulated with 50 ng/ml IGF-I. Cell lysates were collected from serum-starved cells before (0 min) and after stimulation with IGF-I for 5, 15 and 60 minutes. Arrows show the position of the IGF-IR β subunit (95 kDa) and IRS-1 (175 kDa). Protein molecular weight markers are indicated in kDa on the left of the blot. Lower panel: quantification of sample loading by western blot for the IGF-IR.

the IGF-IR kinase on motile behavior of human mammary epithelial cells. For this purpose, we have used parental MCF-7 cells, an MCF-7 cell line overexpressing the wild-type IGF-IR [MCF-7/IGF-IR/WT (Guvakova and Surmacz, 1997)] and novel clonal lines expressing a kinase-dead form of the IGF-IR (designated MCF-7/IGF-IR/DK). Quantitative western blotting was used to compare the level of the IGF-IR in parental MCF-7 cells with clonal lines, which overexpressed either the active or kinase-inactivated IGF-IR. In both transfected cell lines, the receptor was about 20-fold higher than the endogenous level in parental MCF-7 cells (Fig. 1a).

To compare receptor signaling over time in transfected cells, phosphorylation of the IGF-IR and IRS-1 was examined in the wild-type and kinase-dead transfectants treated with IGF-I. Cells expressing the wild-type IGF-IR had higher tyrosine phosphorylation of both the IGF-IRβ subunit and IRS-1 between 5 and 60 minutes following IGF-I treatment. By contrast, MCF-7/IGF-IR/DK cells showed a complete lack of tyrosine phosphorylation of either the IGF-IRβ subunit or IRS-1 (Fig. 1b). These data establish that IGF-IR signaling is blocked in MCF-7/IGF-IR/DK cells at the first step of receptor kinase activation and IRS-1 phosphorylation.

The requirement for the IGF-IR kinase in the disorganization of the epithelial sheet

We next compared migratory behavior of the parental MCF-7 cell line and its derivative clones in response to IGF-I. Parental cells treated with IGF-I became migratory and pulled apart from one another at cell-cell contacts within colonies. Cell surfaces changed markedly, exhibiting intensive membrane ruffling over the apex and at the cell margins. When clones were treated with IGF-I, MCF-7/IGF-IR/WT but not MCF-7/IGF-IR/DK cells developed protrusions, separated from one another and became motile in the direction of intense peripheral ruffling. The MCF-7/IGF-IR/WT cells initially located at the edges of colonies became most motile; these cells detached completely from neighboring cells and migrated freely as single cells until they came into contact with other cells (Movie 1; available at jcs.biologists.org/supplemental**)**.

To estimate the differences in cell migratory behavior in response to IGF-I, we compared ruffling activity and cell movement rates in MCF-7/IGF-IR/WT and MCF-7/IGF-IR/DK cells. Before stimulation, small zones of minor membrane ruffles at the free edges of cells were observed occasionally in both cell types, but apical membrane activity was undetectable. Stimulation with IGF-I resulted in a dramatic increase in the membrane ruffling of MCF-7/IGF-IR/WT over the period of 1 hour and that correlated temporally with cell-cell separation (Fig. 2A). 100% of IGF-I-stimulated MCF-7/IGF-IR/WT cells developed prominent apical membrane activity, and the percentage of cells with peripheral, phase dark ruffling activity doubled (Fig. 2Ba-c). The rates of cell motility were related to the initial position of cells within colonies and varied between 20.7±2.4 μm/hour (mean±s.e.m.) for cells located inside the colonies and 59.7±7.6 μm/hour (mean±s.e.m.) for cells at the periphery of colonies.

In sharp contrast, MCF-7/IGF-IR/DK cells showed no increase in cortical ruffling upon IGF-I stimulation, and less than 20% of MCF-7/IGF-IR/DK cells developed apical membrane protrusions (Fig. 2Bd-f). Furthermore, only 17% of the cells showed any motile activity with mean velocities 3.8±1.6 μm/hour inside the colonies and 13.9±1.9 μm/hour at the colony margins. These results established that in MCF-7 cells IGF-IR tyrosine kinase activity was essential for the formation of apical membrane projections, the increase of lateral ruffling and separation of cells followed by migration.

The IGF-IR kinase regulates concomitant reorganization of α-actinin and F-actin at cell-cell contacts

In MCF-7 cells, the activation of the IGF-IR causes reorganization of the actin cytoskeleton (Guvakova and Surmacz, 1999). Here, we used indirect immunofluoresence to assess whether in separating cells reorganization of F-actin in

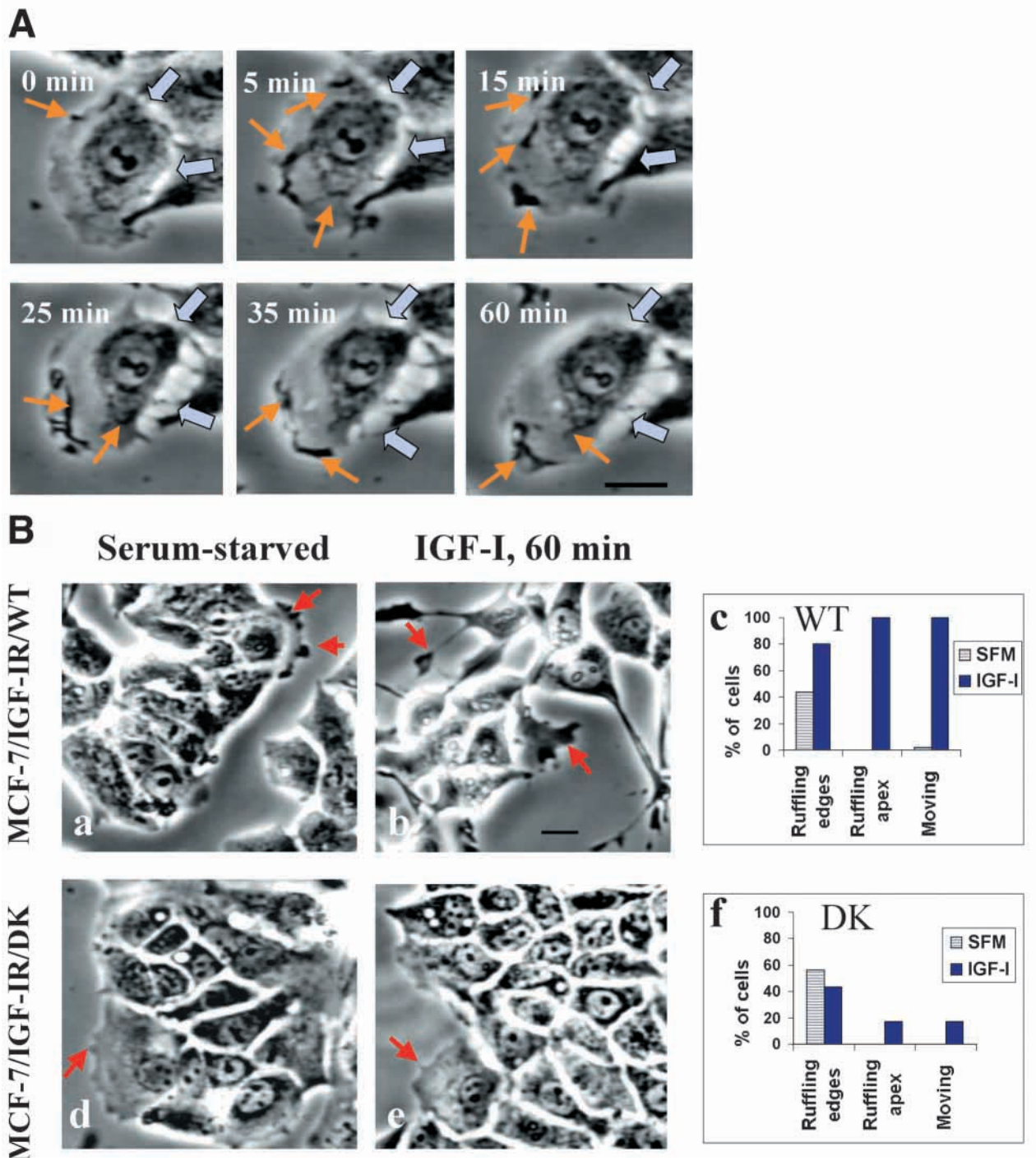

Fig. 2. (A) IGF-I induces membrane ruffling in separating MCF-7/IGF-IR/WT cells. Phase-contrast images of serum-starved MCF-7/IGF-IR/WT cells before and after stimulation with 50 ng/ml IGF-I for indicated times. The thin arrows show examples of apical ruffles. Thick arrows indicate nascent gaps at the sites of cell-cell detachment. Bar, 10 μm. (B) Inhibition of membrane ruffling and cell motility in dead-kinase expressing cells. Phase-contrast images of MCF-7/IGF-IR/WT (a,b) and MCF-7/IGF-IR/DK (d,e) cells. Cells were serum-starved (a,d) or stimulated with 50 ng/ml IGF-I for 60 minutes (b,e). Examples of sporadic lateral ruffles in serum-starved cells are indicated by arrows in a and d. As MCF-7/IGF-IR/WT cells moved apart, they extended long, fine cytoplasmic processes with the lamellipodia at the ends (arrows in b). Bar, 10 μm. (c,f) Quantification of cells with ruffles at free edges and over the cell apex, and migratory cells observed during time-lapse filming in MCF-7/IGF-IR/WT (c) and MCF-7/IGF-IR/DK (f) cells. Cells were incubated overnight in serum-free medium (SFM) and then stimulated with 50 ng/ml IGF-I (IGF-I).

cell-cell contacts is coupled to the distribution of α-catenin and α-actinin, two principle actin-binding proteins that connect microfilaments to adherens junction receptor complexes. In serum-starved MCF-7/IGF-IR/WT cells, α-catenin and α-actinin formed continuous lines along the borders of mature cell-cell contacts, where F-actin was also localized extensively

(Fig. 3Aa,e,i). Within 5 minutes of IGF-I stimulation, about 30-35% of cells had punctuated instead of continuous distribution of α-catenin, which indicated the onset of the disruption of adherens junctions. By contrast, α-actinin appeared highly concentrated at cell margins, and the short actin-enriched projections appeared at cell-cell contacts (Fig. 3Ab,f,j). The formation of the cortical α-actinin and F-actin structures correlated temporally with the loosening of cell-cell contacts and membrane ruffling documented by time-lapse video microscopy. By 15 minutes, the majority of the cells (up to 85%) had discontinuous α-catenin staining at cell-cell borders. In sharp contrast, α-actinin and F-actin continue to highly concentrate within marginal membrane protrusions (Fig. 3Ac,g,k). At 60 minutes, α-catenin localized diffusely in the cytoplasm and in the rare remaining cell-cell contacts, whereas α-actinin and F-actin concentrated at the edges of multiple membrane protrusions (Fig. 3Ad,h,l). These findings indicated that IGF-I-induced separation of MCF-7 cells was associated with the progressive reduction of α-catenin and the increase of α-actinin and F-actin at cell-cell contacts.

The reduction of α-catenin in cell-cell contacts can be achieved experimentally by lowering the concentration of extracellular calcium ions. This process is thought to be associated with unclustering and/or internalization of E-cadherin-catenin complexes (Kusumi et al., 1999). When confluent MCF-7/IGF-IR/WT cells were shifted to PBS containing 0.5 mM EDTA or PBS free of calcium, α-catenin quickly translocated from cell-cell contacts to the cytoplasm before dissociation of the cells. This procedure, however, did not stimulate the assembly of cortical structures containing α-actinin and F-actin or cell motility (data not shown). We propose that IGF-IR-mediated reorganization of the actin cytoskeleton at cell-cell contacts is specific for the process of 'active cell separation' followed by migration as opposed to experimentally induced 'passive cell dissociation' unrelated to cell movement.

To determine the role of the IGF-IR kinase activity in active cell separation, we analyzed the effect of IGF-I on localization of α-actinin and F-actin in MCF-7/IGF-IR/DK cells, in which the dominant-negative receptor no longer activated IGF-IR signaling. In these cells, IGF-I treatment did not alter localization of either α-actinin or F-actin over a 60 minute period (Fig. 3B). The cells continued to have apico-basal polarity and to be organized in tight patches. Thus, in MCF-7 cells, both disorganization of cell-cell contacts and the concomitant concentration of α-actinin and F-actin at cell peripheries are dependent on the catalytic activity of the IGF-IR kinase.

IGF-I activates colocalization of α-actinin with highly ordered actin microspikes

To examine in detail the sites of α-actinin and F-actin colocalization before and after IGF-I stimulation, we used double immunofluorescence staining (Fig. 4A). In serum-starved MCF-7/IGF-IR/WT cells, α-actinin co-distributed with F-actin in a circumferential band, small cytoplasmic aggregates and the tips of the stress fiber-like filaments (Fig. 4Ac). Within 5 minutes of IGF-I stimulation, F-actin appeared to be depleted from the cytoplasm and was instead concentrated in short (~2 μm) bundles that form highly ordered arrays of spikes at cell peripheries (Fig. 4Ad). At the same time, α-actinin showed a striking enhancement in its colocalization with F-actin at the basal portions of actin bundles within microspikes. Notably, there was no α-actinin in the extremities of microspikes where F-actin persisted in the tight bundles (Fig. 4Af). These experiments revealed that IGF-I activates localization of α-actinin at the base of actin microspikes organized in well ordered arrays in lateral zones of separating cells.

To examine more deeply the structure of microspikes in the separating cells, we repeated the IGF-I stimulation experiments, this time processing cells for transmission electron microscropy (TEM). Confluent serum-starved cells had intercellular contacts typical of polarized epithelium (Fig. 4Ba). Within 15 minutes of IGF-I stimulation, finger-like projections formed in the lateral zones of the opposing cells (Fig. 4Bb). That correlated temporally with appearance of α-actinin-actin microspikes identified by immunofluorescence. The average diameter of the membrane-flanked individual projection was 0.24±0.03 μm (mean±s.e.m.), the lengths of projections measured from tip to base varied from 0.27 μm to 1.21 μm. The shorter projections were in close contact with each other, whereas the elongated ones were separated by gaps. Clearly, the core of each projection consisted of a strap of bundled actin oriented perpendicularly to the cell-cell contact zones. Actin bundles traversed projections, extended through the cell body and embedded in the actin meshwork, which coincided well with positioning of the cortical cytoskeleton relatively to the apical membrane and cell nucleus. The average length of the individual actin strap was 1.94±0.15 μm (mean±s.e.m.). That agreed well with the estimated lengths of actin bundles visualized by immunofluorescence. Thus, the ultra-structural analysis confirmed that lateral projections induced by IGF-I in separating cells are actin-enriched microspikes.

In living cells α-actinin microspikes appear as motile apico-lateral structures

To study the dynamics of α-actinin in living cells, we took advantage of confocal laser-scanning microscopy and examined the spatial and temporal effects of IGF-I on full-length α-actinin tagged with EGFP. The interior details from multiple focal planes were recorded as they changed over time (4D imaging). For thorough analysis of α-actinin localization, the representative sections are shown in Fig. 5.

Typically, without IGF-I treatment, α-actinin lined the borders of the adjacent MCF-7/IGF-IR/WT cells. The thin band of α-actinin appeared close to the lateral cell membranes in the most apical optical section and through the cell thickness of 10-12 μm. α-actinin was also localized within small aggregates scattered throughout the cytoplasm and in the fine dotted or streak-like focal structures about 2.5 μm above the substrate surface (Fig. 5Aa,d,g). Once cells were stimulated with IGF-I, the aggregates of α-actinin cleared off the cytoplasm and an increased amount of α-actinin became associated with cell boundaries where the nascent projections were formed. Within a few minutes, the propelling microvilli-like projections containing α-actinin extended and retracted laterally and upward; the most elongated projections (of 6-10 μm in length) bent across the cell apex (Fig. 5Ab,c). The short (of 2-4 μm in length) α-actinin projections were also seen through a series of the middle optical sections spanning 10 μm in height (Fig. 5Ae,f). Within 5 minutes, some cells vanished from view in the most apical sections and then from the series of lateral

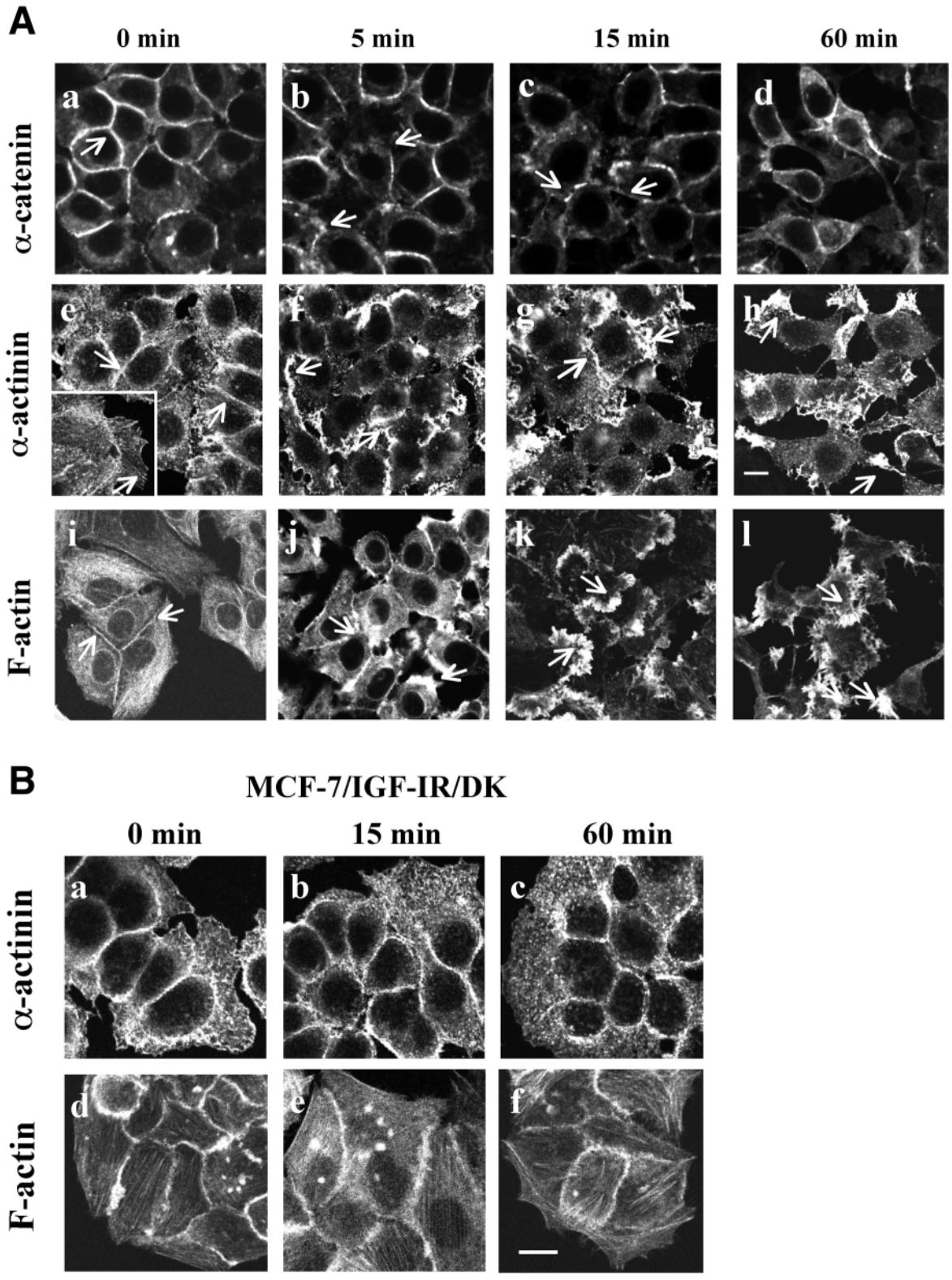

Fig. 3. (A) The effects of IGF-IR activation on redistribution of α-catenin, α-actinin and F-actin. Serum-starved (0 min) MCF-7/IGF-IR/WT cells were treated with 50 ng/ml IGF-I for 5, 15 and 60 minutes, then fixed in 3.7% formaldehyde and stained with a polyclonal antibody to α-catenin (a-d), a monoclonal antibody to α-actinin (e-h) or TRITC-phalloidin for F-actin (i-l). Arrows show examples of α-catenin disappearance from cell-cell contacts (a-c), relocalization of α-actinin to the cellular borders (e-h) and reorganization of F-actin and microspike development (i-l) induced by IGF-I. Inset in e, examples of α-actinin localized at the tips of stress fibers seen at the free edge of the spread cell. Bar, 10 μm. (B**)** IGF-I-stimulated reorganization of α-actinin and F-actin is blocked when the IGF-IR kinase is inactive. Localization of α-actinin (staining with antibody to α-actinin) (a-c) and F-actin (staining with TRITC-phalloidin) (d-f) was examined in MCF-7/IGF-IR/DK cells that were serum starved (0 min) and exposed to 50 ng/ml IGF-I for 5 and 60 minutes. Confocal images are representative of three experiments. Bar, 10 μm.

sections (compare circled areas in Fig. 5Aa with b,d and e). In the same cells, α-actinin motile ruffles formed along the boundaries of the basal membrane. These basal ruffles resembled growth-factor-induced ruffles described in KB cells (Kadowaki et al., 1986). In parallel, the initially minute α-actinin-containing focal structures enlarged and oriented in the direction of cell spreading (Fig. 5Ag-i, circled). By 9 minutes of IGF-I stimulation, these focal structures appeared closer to the substratum than they were in the untreated cells (1.5 μm compared with 2.5 μm from the substrate level). Thus, we found that in separating living cells, α-

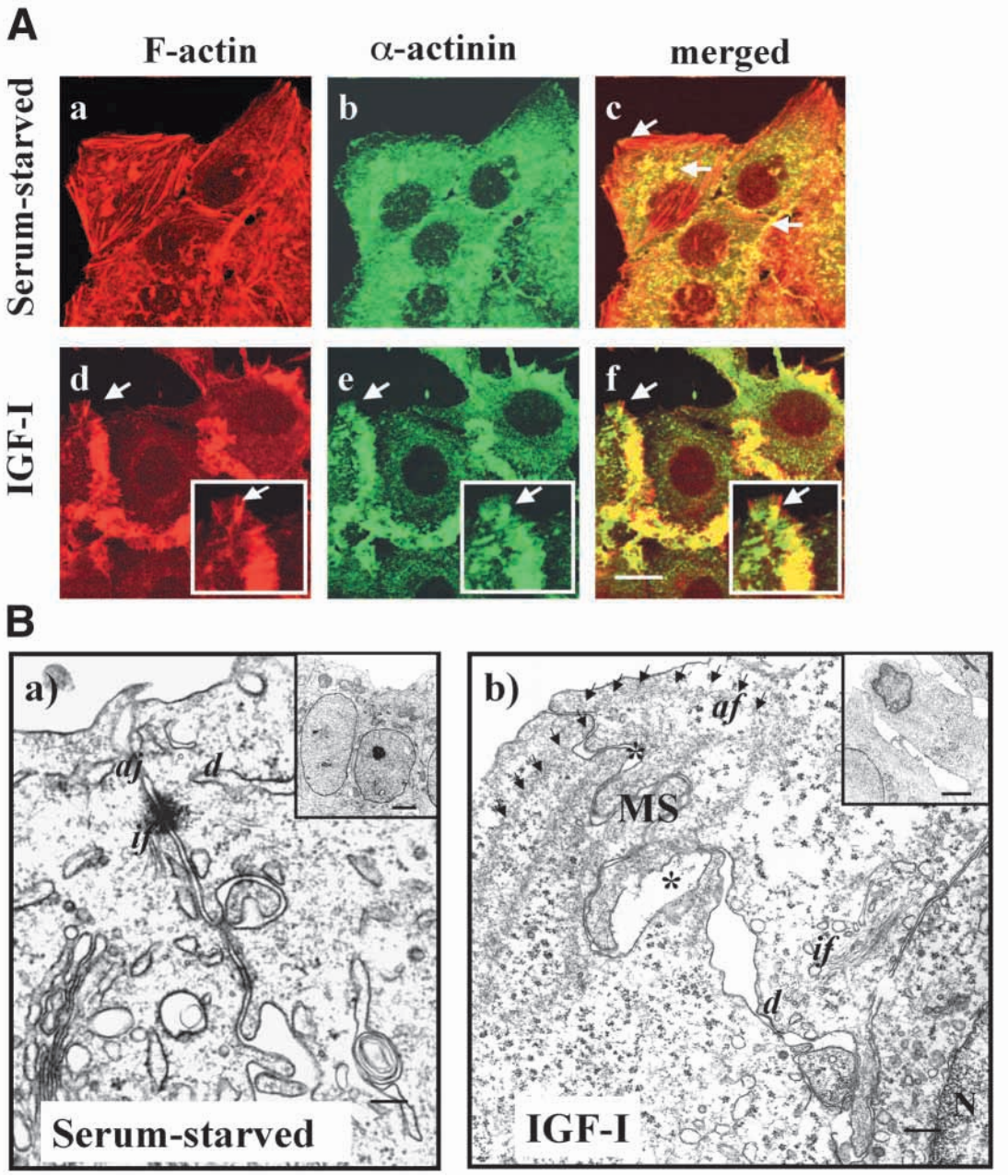

Fig. 4. (A) Colocalization of α-actinin with F-actin in microspikes during IGF-I-induced cell separation. MCF-7/IGF-IR/WT cells, untreated (a-c) or stimulated with 50 ng/ml IGF-I for 5 minutes (d-f), were fixed in 3.7% formaldehyde and co-stained for F-actin with TRITC-phalloidin and for α-actinin with a monoclonal antibody to α-actinin. The images of middle sections acquired by confocal laser-scanning microscopy illustrate staining for F-actin in red (a,d) and α-actinin in green (b,e). In overlays (c,f), sites of α-actinin and F-actin colocalization appear in yellow. Insets in d-f: examples of F-actin and α-actinin-containing microspikes from the zone of the intercellular membrane ruffles pointed to by arrow (d-f). Bar, 10 μm. (B) Ultra-structural analysis of IGF-I-induced microspikes in MCF-7/IGF-IR/WT cells. (a**)** Examples of adherens junction (aj), desmosome (d) and intermediate filaments (if) proximate to desmosomes are indicated in confluent serum-starved cells. The longitudinal section of continuous contacts between lateral membranes is shown in the upper inset. (b**)** Cross-sections through microspikes (MS) formed in the cells stimulated with 50 ng/ml IGF-I for15 minutes. Individual bundles of actin in the core of MS formed by opposing cells are pointed out by a row of arrows; gaps between single microspikes are labeled with asterisks. A membrane site resembling an immature or disassembling desmosome in close proximity to intermediate filaments is labeled d. In the inset, the horizontal section through apical zones of IGF-I-stimulated cells is shown. N, nucleus. Bar, 250 nm. In insets, bar, 5 μm.

actinin is localized in the dynamic apico-lateral microspikes besides focal adhesions and the edges of the basal ruffles.

In MCF-7/IGF-IR/DK cells, despite the continuous treatment with IGF-I, α-actinin remained predominantly localized to lateral membranes of cells tightly adhered to each other. Only minor time-dependent redistribution of α-actinin occurred in the cytoplasm and at the cell borders (Fig. 5B); these changes were typical of all live MCF-7-derived cells regardless of IGF-I stimulation. Taken together these observations clearly show that activation of the IGF-IR causes a time-dependent accumulation of α-actinin-EGFP in the apico-lateral microspikes of separating cells.

The development of α-actinin mutants for molecular genetic analysis of the requirements for α-actinin in microspikes

In the α-actinin molecule, the N-terminal head contains highly conservative actin- and phospholipid-binding sites, the central rod domain is composed of four spectrin-like repeats implicated in dimerization of α-actinin monomers and interaction with other proteins and the C-terminal end of the rod provides binding sites for ions of calcium as well as proteins (Hemmings et al., 1992; Matsudaira, 1994; McGregor et al., 1994; Fukami et al., 1996). The characterization of α-actinin mutants has been particularly difficult in non-muscle cells owing to the rapid lethality of cells expressing the mutant proteins (Scultheiss et al., 1992; Hijikata et al., 1997). To define the contribution of individual domains to the function of α-actinin in microspikes, we have constructed new pEGFP N1-vector-based plasmids encoding the mutant α-actinins as C-terminal chimeras with EGFP (Fig. 6A), and that allowed us to monitor fusion proteins soon after transfection. 230 amino-acid residues in the N-terminus were deleted to yield a mutant α-actinin lacking the entire actin-binding region (ΔN). To inactivate α-actinin in the C-terminus (ΔC), the last 168 amino acids were removed (described in the Materials and Methods).

MCF-7/IGF-IR/WT cells were transfected with plasmid DNA encoding either control EGFP or EGFP chimeras with a full-length wild-type (WT), mutant ΔN and ΔC α-actinin. Cell

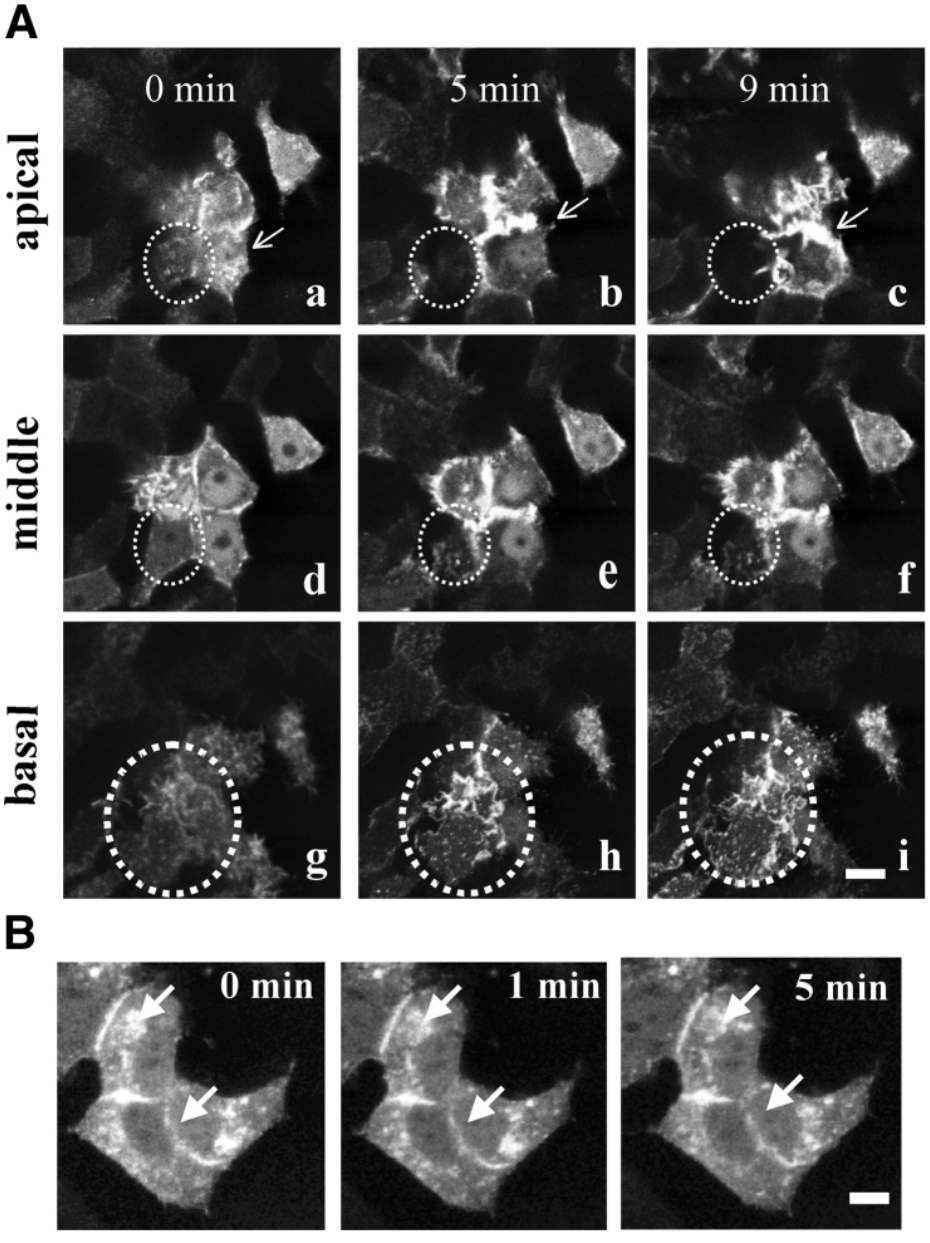

Fig. 5. (A) The development of α-actinin motile projections in living MCF-7/IGF-IR/WT cells stimulated with IGF-I. Dynamics of EGFP-α-actinin in live MCF-7/IGF-IR/WT cells transiently transfected with WT α-actinin-EGFP encoding plasmid. (A-C) The representative laser confocal fluorescence images taken at the apical, middle and basal focal planes in serum-starved cells (a,d,g) stimulated with 50 ng/ml IGF-I for 5 minutes (b,e,h) or for 9 minutes (c,f,i) are shown. Circled is an example of a cell that is flattening, separating and moving from the adjacent cells in response to IGF-I treatment. The optical section from the apical region was taken about 2.0 μm from the top of cells. The example of the lateral single projection that extended and folded over the cell apex is indicated by arrow in a-c. The middle optical sections were collected from the focal plane about 6.5 μm from the top of cells. Basal images were taken close to the substratum level (about 1.5 μm from the glass surface). Bar, 10 μm.
(B) Reorganization of α-actinin is blocked in living MCF-7/IGF-IR/DK cells treated with IGF-I. The images illustrate the localization of α-actinin in live MCF-7/IGF-IR/DK cells transfected with EGFP-labeled α-actinin before (0 min) and after IGF-I stimulation (shown for 1 and 5 minutes). The representative images derived by 3D projection of 20 consecutive apical and middle optical sections are shown. Bar, 10 μm.

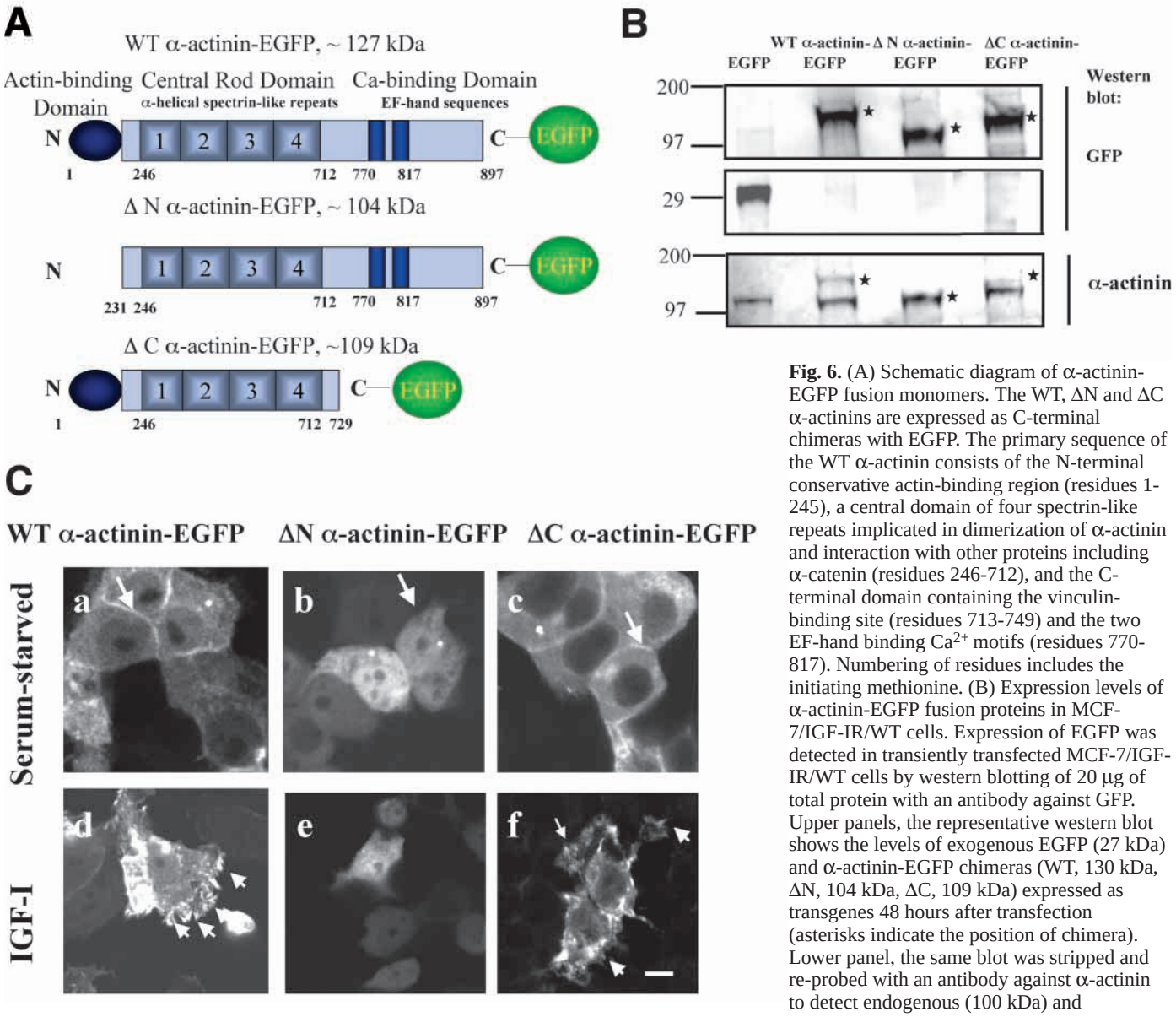

Fig. 6. (A) Schematic diagram of α-actinin-EGFP fusion monomers. The WT, ΔN and ΔC α-actinins are expressed as C-terminal chimeras with EGFP. The primary sequence of the WT α-actinin consists of the N-terminal conservative actin-binding region (residues 1-245), a central domain of four spectrin-like repeats implicated in dimerization of α-actinin and interaction with other proteins including α-catenin (residues 246-712), and the C-terminal domain containing the vinculin-binding site (residues 713-749) and the two EF-hand binding Ca^{2+} motifs (residues 770-817). Numbering of residues includes the initiating methionine. (B) Expression levels of α-actinin-EGFP fusion proteins in MCF-7/IGF-IR/WT cells. Expression of EGFP was detected in transiently transfected MCF-7/IGF-IR/WT cells by western blotting of 20 μg of total protein with an antibody against GFP. Upper panels, the representative western blot shows the levels of exogenous EGFP (27 kDa) and α-actinin-EGFP chimeras (WT, 130 kDa, ΔN, 104 kDa, ΔC, 109 kDa) expressed as transgenes 48 hours after transfection (asterisks indicate the position of chimera). Lower panel, the same blot was stripped and re-probed with an antibody against α-actinin to detect endogenous (100 kDa) and exogenous EGFP-α-actinins whose positions on the blot are indicated by asterisks. Note that the endogenous α-actinin and ΔN α-actinin-EGFP overrun in a 100 kDa band. (C) Intracellular localization of WT, ΔN, ΔC α-actinin-EGFP fusion proteins in serum-starved and IGF-I-stimulated MCF-7/IGF-IR/WT cells. MCF-7/IGF-IR WT cells were transfected with plasmid encoding WT or ΔN or ΔC α-actinin-EGFP. 24 hours after transfection, serum-starved cells were either fixed in 3.7% formaldehyde (a-c) or stimulated with 50 ng/ml IGF-I for 15 minutes and then fixed (d-f). The representative images of the middle optical sections acquired by confocal laser-scanning microscopy show (top panel, a-c) the WT and ΔC α-actinins incorporated into the mature cell-cell junctions (pointed by arrow) and ΔN α-actinin stained in the cytoplasm and nucleus. Lower panel, d-f: the images show the formation of α-actinin-EGFP-containing spikes (arrows in d); diffuse staining for ΔN α-actinin-EGFP (e), aggregation of ΔC α-actinin-EGFP and formation of the defective microspikes (f). Bar, 10 μm.

extracts were resolved electrophoretically, and proteins transferred on the membrane were probed sequentially with antibody to GFP and α-actinin. Western immunoblotting has confirmed protein expression and the expected molecular weights of exogenous EGFP (27 kDa), WT (127 kDa), ΔN (104 kDa) and ΔC (109 kDa) EGFP-α-actinins (Fig. 6B).

Both head and tail domains of a-actinin are required for the development of highly ordered microspikes

To visualize the dynamics of α-actinin-EGFP fusion proteins specific to the regions of cell-cell contacts, we used confocal laser-scanning microscopy and collected stacks of images from the middle optical sections crossing nuclei. In serum-starved cells with mature cell-cell contacts, only the wild-type and ΔC α-actinins incorporated into pre-existing cell-cell junctions. Unlike the wild-type and ΔC α-actinin, ΔN α-actinin did not associate with the circumferential actin ring and was instead localized diffusely throughout the cell body (Fig. 6Ca-c).

In WT α-actinin transfectants, IGF-I triggered the expected reorganization of cell-cell contacts and the assembly of α-actinin-actin microspikes in the lateral zones (Fig. 6Cd).

Table 1. Effects of α-actinin mutants on microspikes

DNA, transfected	Total cells counted, *n*	Cells transfected, %*	Cells with α-actinin/actin spikes, %**
Wild-type α-actinin	173	46.2±3.6	31.0±3.2
ΔN α-actinin	183	39.7±3.3	0.0±0.0
ΔC α-actinin	159	39.5±3.8	14.4±5.0

Deletion of the N-terminal head region prevents incorporation of α-actinin into microspikes, whereas deletion of the C-terminal tail region inhibits formation and distribution of microspikes at the cellular borders.

*% of total counted cells, **% of transfected EGFP-positive cells.

Values are means±s.e.m. from five random fields in two independent experiments.

ΔN α-actinin did not colocalize with actin microspikes and remained diffused throughout the cell body (Fig. 6Ce). The number of ΔC α-actinin-transfected cells with α-actinin-actin spikes was half that of wild-type transfectants. Moreover, the spatial relationship between ΔC α-actinin and F-actin was disturbed, as microspikes did not organize into well ordered arrays (Fig. 6Cf). In two independent experiments, the appearance of microspikes was assessed quantitatively (Table 1). Collectively, these results demonstrate that in the α-actinin molecule both the head and tail regions are required for the function of microspikes. The N-terminal part of α-actinin is necessary for association of α-actinin with actin bundles, whereas the C-terminal tail of the rod is needed for correct assembly and/or positioning of microspikes at cell peripheries.

The mechanism of active cell separation and microspike assembly requires activities of PI 3-kinase-generated phospholipids

To address the role of IGF-IR kinase signaling in regulating microspike assembly in relation to cell separation, we used four specific pharmacological inhibitors of PI 3-kinase and MAP kinase signaling pathways (Fig. 7). They are LY 294002, a specific inhibitor of the catalytic subunit of the PI 3-kinase; a D3-modified phosphatidylinositol (PI) ether lipid analog (also called Akt inhibitor); PD 98059, a synthetic inhibitor of the MAP kinase-activating enzyme, MAPK/ERK kinase (MEK1); and UO 126, an inhibitor of MEK1 and MEK2. In MCF-7/IGF-IR/WT cells treated with LY 294002, the normal induction of phosphorylation of the PKB/Akt by putative PDK2 on serine 473 was downregulated by 90% and 84% and by 3-phosphoinositide-dependent kinase 1 (PDK1) on threonine 308 by 28% and 20%, and at 5 and 15 minutes, respectively. The 3D-modified PI-analog also downregulated signaling associated with the activities of PI 3-kinase-generated phospholipids, although its effect on phosphorylation of PKB/Akt was much less. The relative phosphorylation of PKB/Akt on serine 437 was reduced by 8% and 19%, and on threonine 308 by 9% and 11% at 5 and 15 minutes of IGF-I stimulation (average of five experiments) (Fig. 7a). PD 98059 reduced the relative phosphorylation of ERK1/2 MAP kinases on threonine 202 and tyrosine 204 by 73% and 67% at 5 and 15 minutes of IGF-I treatment (average of four experiments). UO 126 was a much more potent inhibitor of ERK1/2 MAPK kinases; it blocked completely IGF-I-stimulated and basal phosphorylation of these kinases (Fig. 7b and data not shown).

Pretreatment of MCF-7/IGF-IR/WT cells with 10 μM LY294002 and 40 μM PI analog before the addition of 50 ng/ml IGF-I blocked the formation of cortical microspikes and cell separation in response to IGF-I [compare Fig. 8A,b with c,d also with Guvakova et al. (Guvakova et al., 2002)]. LY 294002- and PI-analog-pretreated cells remained organized in tight colonies during at least 60 and 30 minutes of the IGF-I treatment, respectively. By contrast, there was no apparent inhibitory effect of 50 μM PD 98059 on cell separation; cells, exposed to this drug or not, appeared spindle-shaped, separated from each other and migrated within 60 minutes of IGF-I stimulation. The formation of well ordered α-actinin-actin microspikes was slightly disturbed by PD 98059 (compare Fig. 8A,b with e). The more potent inhibitor of MEK1 and MEK2, UO 126, did not prevent IGF-stimulated concentration of α-actinin and actin in the peripheral microspikes (Fig. 8Af); however, it inhibited cell migration radically within first 60 minutes of IGF-I stimulation (data not shown).

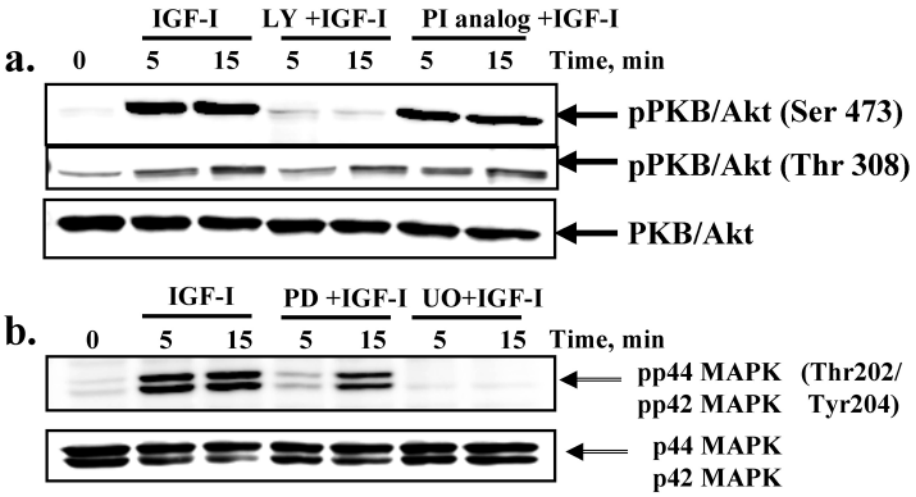

Fig. 7. Effects of inhibitors on IGF-I-induced activation of the PI 3-kinase and MAP kinase signaling pathways. (a) Serum-starved cells (0). Cells not exposed to inhibitors (IGF-I) and pre-treated with 10 μM LY 294002 for 30 minutes (LY+IGF-I) or 40 μM PI analog for 3 hours (PI analog+IGF-I) were stimulated with 50 ng/ml IGF-I for the indicated times. Phosphorylation of PKB/Akt was detected with an antibody against phospho-Akt. For a loading control, the same blots were stripped and re-probed with an antibody against Akt (Materials and Methods). One of the re-probed blots is shown. (b). Serum-starved cells (0). Cells not exposed to inhibitors (IGF-I) and pre-treated with 50 μM PD 98059 (PD+IGF-I) or 50 μM UO 126 (UO+IGF-I) for 30 minutes were stimulated with 50 ng/ml IGF-I for the indicated times. The ERK1/2 MAPK phosphorylation was detected with specific phospho-MAPK antibodies. The same blot was stripped and re-probed with antibody against total ERK1/ERK2 (p44/p42) (Materials and Methods).

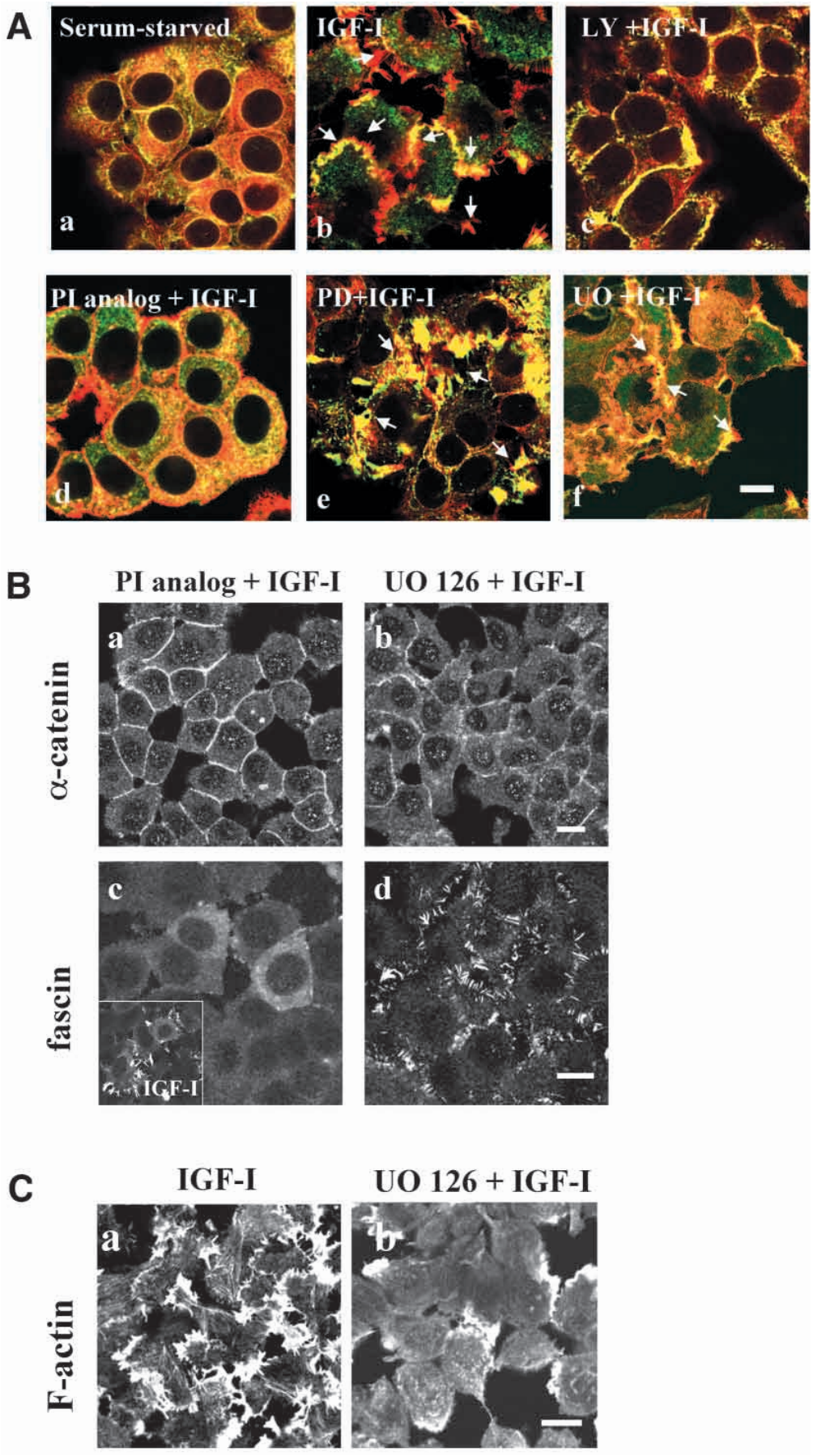

Fig. 8. A. The development of α-actinin/actin microspikes by IGF-I is blocked by the inhibitors of PI-3 kinase signaling. MCF-7/IGF-IR/WT cells were serum-starved (a), serum-starved and then stimulated with 50 ng/ml IGF-I for 15 minutes (b), pre-treated for 30 minutes with 10 μM LY 294002 (c), for 3 hours with 40 μM D3-PI analog (d), 30 minutes with 50 μM PD 98059 (e) or 30 minutes with 50 μM UO 126 (f) and then stimulated with 50 ng/ml IGF-I for 15 minutes. (a-f) Overlays of confocal images of cells stained with TRITC-phalloidin (red) and antibody against α-actinin (green). Examples of actin/α-actinin microspikes are indicated by arrows. Images are representative of three experiments. Bar, 10 μm. (B) Differential effects of the PI analog and UO 126 on IGF-I-stimulated loss of adherens junctions and formation of microspikes. Serum-starved MCF-7/IGF-IR/WT cells were pretreated with 40 μM D3-PI analog for 3 hours, stimulated with 50 ng/ml IGF-I for 15 minutes in the presence of the inhibitor, fixed and stained with antibody to α-catenin (a) or fascin (c) (Materials and Methods). In parallel, the same serum-starved cells were pretreated with 50 μM UO 126 for 30 minutes, stimulated with 50 ng/ml IGF-I for 15 minutes, then fixed and stained with an antibody to α-catenin (b) or fascin (d). The relocation of α-catenin from adherens junctions normally induced by IGF-I (compare with Fig. 3Aa-d) is blocked by the PI analog but not UO 126. Normal stimulation of fascin microspikes by IGF-I (inset in c, 50 ng/ml IGF-I, 15 minutes) is also blocked only by the PI analog. Confocal images are representative of four independent experiments. Bar, 10 μm. (C) The MEK1/2 inhibitor affects function of stress fibers in IGF-I-stimulated cells. Serum-starved cells not exposed to inhibitor (a) or pretreated with 50 μM UO 126 for 30 minutes (b) were stimulated with 50 ng/ml IGF-I for 15 minutes, then fixed and stained with TRITC-phalloidin. IGF-I normally promotes disassembly of stress fibers within 5 minutes followed by their re-assembly typically after 15 minutes. In cells pretreated with the MEK1/2 inhibitor, re-assembly of the prominent stress fibers is markedly inhibited. The representative images of optical sections collected at the basal level of the cells are shown. Bar, 10 μm.

MEK1/2 signaling downstream of the IGF-IR kinase is essential for migration of separated cells

The above findings prompted our suggestion that MEK1/2 signaling is unnecessary for initial steps of cell-cell separation but may be essential for movement of the cells separated in response to PI 3-kinase signaling. To test this idea, we compared the effect of the PI analog and UO 126 on IGF-stimulated reorganization of cell-cell contacts, this time monitoring distribution of α-catenin, a molecular marker of adherens junctions, and fascin, a marker of the peripheral actin microspikes. In contrast to α-actinin, fascin localizes along the length of actin bundles induced by IGF-I and that allows visualizing microspikes without co-staining for F-actin (Guvakova et al., 2002). Pretreatment of cells with the PI analog blocked IGF-I-stimulated redistribution of α-catenin and thereby dissolution of adherens junctions. This inhibitor also blocked the formation of microspikes containing fascin (Fig. 8Ba,c; inset in c, fascin microspikes induced by IGF-I). In sharp contrast, total inhibition of MEK1/2 activity by UO 126 did not prevent a loss of α-catenin from adherens junctions and did not block the formation of fascin microspikes at cell peripheries (Fig. 8Bb,d). Strikingly, inhibition of MEK1/2 by UO 126 had a marked effect on stress fibers. Normally, activation of the IGF-IR in MCF-7 cells results in a rapid disassembly of stress fibers followed by re-assembly of microfilaments after 15 minutes of IGF-I stimulation. The latter coincides with advancing long protrusions and moving the cell body [seen in Fig. 3Ai-l and described in detail in (Guvakova and Surmacz, 1999)]. Pretreatment with UO 126 had no effect on disassembly of stress fibers; however, it prevented their re-assembly as well as the development of the long membrane protrusions after 15 minutes of IGF-I stimulation (compare Fig. 8Ca with b).

We conclude that separation of MCF-7 breast cancer cells in response to IGF-I is dependent on signaling from the activated IGF-IR through the PI 3-kinase and its phospholipid products, and that signaling through MEK1/2 may be necessary for subsequent cell locomotion.

Discussion

The IGF system is essential for normal development of the mammary gland, and its disruption in human breast cancer leads to an excess of IGF-IR signaling. The biological relevance of the enhanced catalytic activity of the IGF-IR kinase to breast tumor progression has not been established. In this study, using a combination of molecular genetic, biochemical and pharmacological approaches with a complementary monitoring of living cell behavior, we have identified a novel mechanism by which the IGF-IR kinase induces separation and migration of human breast carcinoma cells.

Cell motile responses mediated by the IGF-IR

It has previously been established that polypeptide growth factors acting through receptor tyrosine kinases can induce transition of cells from an epithelial to a motile fibroblastic phenotype, a phenomenon that resembles epithelial-mesenchymal transition, which occurs during development (Boyer and Thiery, 1993). IGF-I is mainly known as a mitogenic growth factor, and signaling through the IGF-IR in mammary epithelial cells has been chiefly studied in respect to effects on cell proliferation and apoptosis (reviewed by Lee et al., 1998; Chernicky et al., 2000). Nevertheless, a role for the IGF-IR in motility of breast carcinoma cells had been proposed more than a decade ago on the basis of the results of the Boyden chamber assay (Kohn et al., 1990). It should be noted, however, that in this assay cells are artificially separated from each other before examination, and it is therefore not possible to analyze mechanisms of epithelial sheet disintegration.

In this study we examined in detail the effects of IGF-I on motile behavior of cells within an epithelial sheet. We have now demonstrated that, like other growth factors with scattering function, IGF-I induced cell motile responses in a biphasic manner, first causing separation and subsequently causing migration of the cells. The phase of active separation lasted only for 15-30 minutes and was unusually short compared with the 5-16 hours reported for HGF/SF, FGF-1 and EGF (Stoker and Perryman, 1985; Savagner et al., 1997; Müller et al., 1999). During the separation phase, IGF-I stimulated highly dynamic activity of the entire cellular membrane: formation of apical ruffles and motile apico-lateral microspikes, dissolution of adherence junctions and an increase in basal membrane ruffling. Although the precise mechanism of such rapid morphological alterations is unknown, the appearance of dynamic microspikes at the cell-cell contacts and temporal correlation of this event with disintegration the adherens junction complex led us to suggest that microspikes facilitate cell-cell detachment. In addition to acute cell separation, video tracking has revealed uncommonly fast rates of migration of single MCF-7/IGF-IR/WT cells. Collectively these data establish for the first time that activation of the IGF-IR can in the short-term cause destabilization of cell-cell interactions, leading to quick separation and migration of breast cancer epithelial cells.

IGF-IR-mediated active cell separation: structural reorganizations

EGF modulates the interaction between the adherens junction receptor E-cadherin and the actin cytoskeleton, although associated cytoskeletal reorganizations have not been characterized (Hazan and Norton, 1998). Our previous work has shown that in MCF-7 cells, IGF-I induces rapid disassembly of stress fibers and extensive reorganization of the cortical actin (Guvakova and Surmacz, 1999). We have now demonstrated that disassembly of the cortical actin belt coincides with mobilization of α-actinin and actin into apico-lateral microspikes and displacement of α-catenin from the adherens junctions. This agreed with the recent report that activation of the IGF-IR induces redistribution of E-cadherin and β-catenin from the adherens junctions into the cytoplasm (Morali et al., 2001).

What drives α-actinin into cell-cell contacts? As an actin-binding protein, intact α-actinin shows a prominent colocalization with filamentous actin. Yet α-actinin can bind to a number of molecules, in addition to actin (Crawford et al., 1992; Otey et al., 1993; Kroemker et al., 1994; McGregor et al.,1994; Christerson et al., 1999) that perhaps determine the localization of α-actinin. For example, in Cos and PtK2 cells, mutated α-actinins with a deleted actin-binding site were not

incorporated into stress fibers, although they localized to ruffled membranes and adherens junctions (Hemmings et al., 1992; Hijikata et al., 1997). The prominent localization of α-actinin to adherens junction has been related to the direct association between the central rod domain of α-actinin and the C-terminus of α-catenin (Knudsen et al., 1995; Nieset et al., 1997). In epithelial culture, α-actinin colocalizes with vinculin and the cadherin-catenin complex. In this study, we used GFP-labeled α-actinin to follow distribution of α-actinin in living cells before and after IGF-I stimulation. Our results with a GFP-labeled mutant of α-actinin, in which the α-catenin-binding site was preserved while the actin-binding domain was removed, support the idea that both α-catenin and actin-binding sites of α-actinin are essential for localization of this protein into the mature cell-cell junctions. The interaction of the C-terminal end of α-actinin with vinculin does not seem to be required because a GFP-tagged ΔC α-actinin mutant in which the vinculin-binding site was disrupted did not interfere with the ability of α-actinin to localize to intercellular junctions. The development of microspikes in response to IGF-I required at least two fully functional regions of the α-actinin molecule. As expected, the head of α-actinin was obligatory for binding to actin spikes. The C-terminal tail of α-actinin was required for correct assembly and/or stabilization of microspikes because the truncation of this region reduced the number of α-actinin/actin microspikes and caused their misalignment at the cell periphery. According to the previous suggestion, it is possible that the actin-binding activity of α-actinin requires a ternary interaction with the C-tail as modifications in the EF-hand domain of α-actinin have deleterious effects on the activity of its actin-binding domain (Witke et al., 1993; Dubreuil and Wang, 2000). Additionally, direct interaction of α-actinin with vinculin, which is probably disturbed in the ΔC α-actinin mutant, might be required for correct organization of microspikes. Thus our findings establish that functional α-actinin is necessary for the development of microspikes and is not passively reorganized following actin.

Our results, while supporting previous findings on IGF-I-stimulated actin polymerization at the cell periphery (Kadowaki et al., 1986; Isumi et al., 1988), further demonstrate that activation of the IGF-IR coordinates reorganization of actin into peripheral microspikes. Localization of α-actinin at the base rather than at the tips of microspikes implies that other actin-crosslinking protein(s) compose the core of a spike. A good candidate for this role is the 55 kDa actin-bundling protein fascin, which acts as a crosslinker, causing aggregation of actin into tight bundles (Edwards and Bryan, 1995; Kureishy et al., 2002). In vitro, fascin and α-actinin synergistically affect mechanical properties of actin filaments (Tseng et al., 2001). In vivo, fascin plays a role in extending the membrane during cell spreading and migration, and overexpression of fascin in pig epithelial cells caused the disorganization of cell-cell contacts (Yamashiro et al., 1998). Fascin also acts as a negative regulator of cell-cell interactions in rat mammary epithelial cells (Wong et al., 1999). Activation of the IGF-IR in MCF-7 cells induces rapid relocalization of fascin from the cytoplasm to the peripheral actin microspikes (Guvakova et al., 2002). We reason now that the activated IGF-IR induces cortical actin dynamics beneath the plasma membrane by increasing actin polymerization and promoting crosslinking of actin by fascin to stabilize the cores of microspikes and by α-actinin to properly position these nascent projections at the cell periphery. Although the significance of microspikes in cell-cell separation remains hypothetical, one possibility is that microspikes play an active cytomechanical role in the destabilization of interactions between opposing cells. Alternatively, microspikes may be the form of cell-cell contacts that are transient and more flexible than adherens junctions and therefore provide the intermediate strength of adhesion between separating cells.

IGF-IR-regulated cell motility: signaling pathways

Cell-cell detachment and microspike formation was completely blocked in MCF-7/IGF-IR/DK cells, clearly indicating the direct causative relationship between IGF-IR activation and α-actinin redistribution. Although it is conceivable that IGF-IR signaling affects the phosphorylation status of α-actinin, at least two lines of evidence imply that tyrosine phosphorylation of α-actinin is not relevant to the development of microspikes in MCF-7 cells. First, there was no detectable difference in the tyrosine phosphorylation of α-actinin immunoprecipitated from cells stimulated with IGF-I (see Materials and Methods). Second, the WT α-actinin-EGFP chimera, which lacked the only identified phopshotyrosine residue 12 within the amino-acid motif QTNDY (Izaguirre et al., 2001), was nevertheless functionally active and localized to microspikes.

As relocalization of α-actinin into cortical structures was detected after 1-2 minutes of IGF-I stimulation, we predicted that the early signaling triggered by the ligand-receptor interaction promotes the development of microspikes. In MCF-7 cells, activation of the IGF-IR kinase quickly drives the formation of a complex between the receptor and substrates IRS and Shc that brings about activation of the downstream cascades of serine/threonine kinases and the PI 3-kinase. Interestingly, in different epithelial cells, different kinases play roles in cell motility. In MDCK canine epithelial cells, activation of both the PI 3-kinase and MAP kinase was found to be essential for the motile response to HGF/SF (Royal and Park, 1995; Potempa and Ridley, 1998). The function of MAP kinases was delineated in scattering triggered by HGF/SF in HT29 colon carcinoma cells and haptotaxis in FG carcinoma cells and T47D breast carcinoma cells (Klemke et al., 1997; Herrera, 1998; Spencer et al., 2000), whereas pretreatment with the MEK1 inhibitor, PD 98059, was dispensable for the chemotactic response of MCF-7 cells to IGF-I (Manes et al., 1999). Others have reported that IGF-I stimulates colonic epithelial cell migration in a wound healing assay through multiple signaling pathways including PI 3-kinase, MAP kinases and PKC-γ and -δ (Andre et al., 1999). In MCF-7 cells expressing the dominant-negative receptors, activity of the PI-3 and the ERK1/2 MAP kinases is downregulated via markedly reduced signaling through IRS-1 and Shc pathways (in this paper and M.A.G., unpublished). To dissect signaling pathways essential for cell motility, we applied selective pharmacological inhibitors of PI 3-kinase and MEK. The MEK inhibitor also inhibits ERK1/2 MAP kinases (summarized in Fig. 9a). Using immunofluorescence staining coupled with biochemical analysis, we found that the activity of PI 3-kinase rather than that of the MAP kinases was required for disassembly of adherens junctions and redistribution of actin,

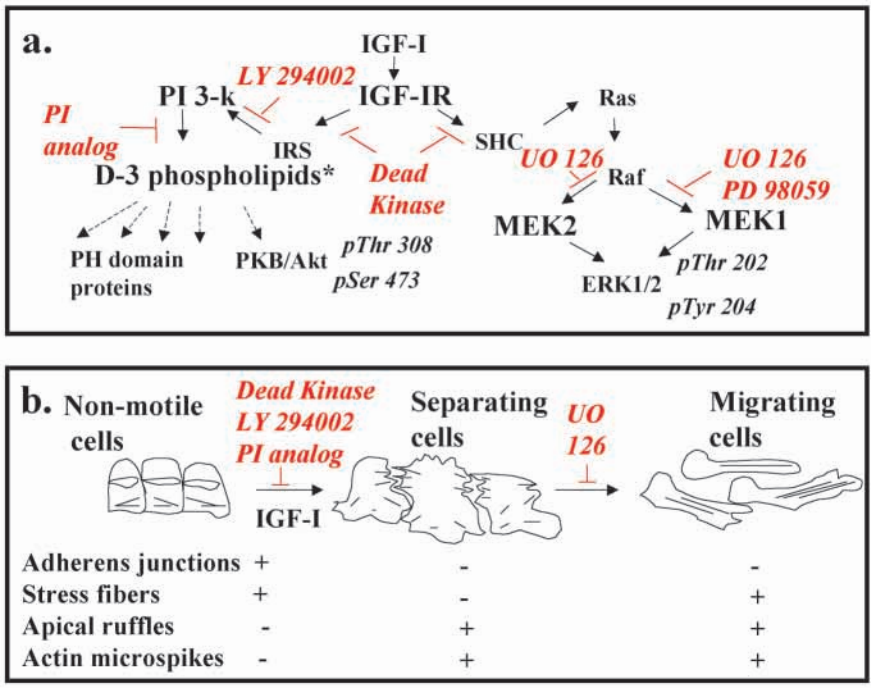

Fig. 9. (a) Scheme showing which IGF-IR signaling pathways were blocked using a molecular genetic approach (dead kinase IGF-IR) and the pharmacological compounds LY 294002, UO 126, PD 98059 and PI analog. *D3 phospholipids: PtdIns(3)*P*, PtdIns(3,4)P_2, PtdIns(3,5)P_2, PtdIns(3,4,5)P_2; (b) A model of biphasic motility responses regulated by the IGF-IR kinase in MCF-7 cells. Non-motile polarized epithelial cells develop mature adherens junctions and prominent stress fibers; apical ruffles and actin microspikes are not present. The initial stage of cell motility, active cell separation, is characterized by a loss of adherens junctions, disassembly of stress fibers, increased membrane ruffling and formation of actin microspikes; these processes are blocked by the inhibitors of the PI 3-kinase but not of MEK1/2 signaling. The subsequent transition of the cells from separating to migrating is characterized by re-assembly of stress fibers, development of the long membrane protrusions and translocation of the cell body over substratum. MEK1/2 inhibitor blocks all these processes.

α-actinin and fascin into microspikes during cell separation. Subsequently, the activity of MEK1/2 appeared to be necessary for re-assembly of stress fibers, which may be involved in the extension of cell protrusions and the translocation of the cell body (model in Fig. 9b). As activities of the ERK1/2 MAP kinases may enhance myosin light chain kinase (MLCK) activity, leading to the phosphorylation of myosin light chains (MLC) (Klemke et al., 1997), it seems possible that IGF-IR signaling sequentially coordinates cell-cell separation and phospho-MLC-dependent cytoskeletal contraction culminating in cell movement.

The function of the PI 3-kinase targets implicated in actin reorganization is dependent on PI 3-kinase-generated phospholipids (Nobes et al., 1995). Moreover, α-actinin may bind to the PI kinase and its product, phosphatidylinositol (3,4,5)-trisphosphate [PtdIns(3,4,5)P_3] (Shibasaki et al., 1994; Greenwood et al., 2000). To investigate the role of PI-3-kinase-generated phosphatidylinositides in cell separation, we used a D3-modified PI analog, a competitive inhibitor of the PI 3-kinase with respect to PI, synthesized to selectively block the effect of myo-inositol-derived second messengers of the PI 3-kinase (Hu et al., 2000). This compound prevented a loss of α-catenin from adherens junctions as prevented redistribution of α-actinin and fascin into actin microspikes, suggesting a role for D3 phospholipids in IGF-I-stimulated cell separation. Although PKB/Akt possesses a pleckstrin-homology (PH) domain and may bind to PI-3-kinase-generated phospholipids, its phosphorylation in MCF-7 cells was only slightly reduced by the PI analog. Thus, the precise role of this kinase as well as other proteins bearing PH domains, including several adaptor proteins and GTP/GDP exchange and GTP-activating proteins for the ARF/Rho/Rac family of GTP-binding proteins, has yet to be investigated.

In summary, we have identified the first biochemically defined pathway in which the IGF-IR tyrosine kinase, through activities of the PI 3-kinase and α-actinin, promotes active separation in human breast cancer cells. We have also established the requirement for MEK1/2 activity in IGF-IR-mediated movement of these cells. Further development of α-actinin mutants and the measurements of the direct association between α-actinin and other molecules in living cells should make it possible to understand the dynamic regulation of microspikes and their role in cell separation. Further studies are needed to reveal the precise mechanisms by which MAP kinases control motility in the separated breast cancer cells.

We are very grateful to Derek LeRoith (NIH) for providing the mutant IGF-IR cDNA, Joseph Sanger (University of Pennsylvania) for the generous gift of EGFP-α-actinin encoding plasmid, and Lewis Tilney (University of Pennsylvania) for expertise for the actin study. We thank Mark Shipman for assistance and advice with use of Improvision software, image processing and movie production, Irina Chernysh for help with use of the LaserSharp 2000 software for 4D imaging in live cells and Patricia Connelly for excellent technical assistance with TEM. We would especially like to thank Francois Huber for discussing strategies on the DNA construct design and Laura Lynch for critical comments on the manuscript. This work was supported by the Breast Cancer Research Program of the Department of Defense DAMD 17-97-1-7211 award (to M.A.G.), National Institute of Health grant CA 16502 (to D.B.), and Wellcome Trust grant 038284 (to J.C.A.).

References

Andre, F., Rigot, V., Remacle-Bonnet, M., Luis, J., Pommier, G. and Marvaldi, J. (1999). Protein kinase C-gamma and -delta are involved in insulin-like growth factor I-induced migration of colonic epithelial cells. *Gastroenterology* **116**, 64-77.

Baron, M. D., Davison, M. D., Jones, P. and Critchley, D. R. (1987). The sequence of chick α-actinin reveals homologies to spectrin and calmodulin. *J. Biol. Chem.* **262**, 17623-17629.

Baserga, R. (1999). The IGF-I receptor in cancer research. *Exp. Cell Res.* **253**, 1-6.

Boyer, B. and Thiery, J.-P. (1993). Epithelium-mesenchyme interconversions as example of epithelial plasticity. *APMIS* **101**, 257-268.

Chausovsky, A., Tsarfaty, I., Kam, Z., Yarden, Y., Geiger, B. and

Bershadsky, A. D. (1998). Morphogenetic effects of neuregulin (neu differentiation factor) in cultured epithelial cells. *Mol. Biol. Cell* **9**, 3195-3209.

Chernicky, C. L., Yi, L., Tan, H., Gan, S. U. and Ilan, J. (2000). Treatment of human breast cancer cells with antisense RNA to the type I insulin-like growth receptor inhibits cell growth, suppresses tumorigenesis, alters the metastatic potential, and prolongs survival in vivo. *Cancer Gene Ther.* **7**, 384-395.

Christerson, L. B., Vanderbilt, C. A. and Cobb, M. H. (1999). MEKK1 interacts with alpha-actinin and localizes to stress fibers and focal adhesions. *Cell Motil. Cytoskeleton* **43**, 186-198.

Cowin, P. and Burke, B. (1996). Cytoskeleton-membrane interactions. *Curr. Opin. Cell Biol.* **8**, 56-65.

Crawford, A. W., Michelsen, J. W. and Beckerle, M. C. (1992). An interaction between zyxin and α-actinin. *J. Cell Biol.* **116**, 1381-1393.

Davies, J. A. and Garrod, D. R. (1997). Molecular aspects of the epithelial phenotype. *BioEssays* **19**, 699-704.

Dabiri, G. A., Turnacioglu, K. K., Sanger, J. M. and Sanger, J. M. (1997). Myofibrillogenes is visualized in living embryonic cardiomyocytes. *Proc. Natl. Acad. Sci. USA* **94**, 9493-9498.

Doerr, M. E. and Jones, J. I. (1996). The roles of integrins and extracellular matrix proteins in the insulin-like growth factor I-stimulated chemotaxis of human breast cancer cells. *J. Biol. Chem.* **271**, 2443-2447.

Dubreuil, R. R. and Wang, P. (2000). Genetic analysis of the requirements for α-actinin function. *J. Muscle Res. Cell Motil.* **21**, 705-713.

Edwards, R. A. and Bryan, J. (1995). Fascins, a family of actin bundling proteins. *Cell Motil. Cytoskeleton* **32**, 1-9.

Firon, M., Shahrabany, M., Altstock, R. T., Horev, J., Abramovici, A., Resau, J. H., Vande Woude, G. F., and Tsarfaty, I. (2000). Dominant negative Met reduces tumorigenicity-metastasis and increases tubule formation in mammary cells. *Oncogene* **19**, 2386-2397.

Furge, K. A., Zhang, Y. W. and Vande Woude, G. F. (2000). Met receptor tyrosine kinase: enhanced signaling through adapter proteins. *Oncogene* **19**, 5582-5589.

Fukami, K., Sawada, N., Endo, T. and Takenawa, T. (1996). Identification of a phosphatidylinositol 4,5-bisphosphate-binding site in chicken skeletal muscle α-actinin. *J. Biol. Chem.* **271**, 2646-2650.

Greenwood, J. A., Theibert, A. B., Prestwich, G. D. and Murphy-Ullrich, J. E. (2000). Restructuring of focal adhesion plaques by PI 3-kinase: Regulation by PtdIns (3,4,5)-P_3 binding to α-actinin. *J. Cell Biol*. **150**, 627-641.

Gumbiner, B. M. (1996). Cell adhesion: the molecular basis of tissue architecture and morphogenesis. *Cell* **84**, 345-357.

Gumbiner, B. M. (2000). Regulation of cadherin adhesive activity. *J. Cell Biol.* **148**, 399-404.

Guvakova, M. A. and Surmacz, E. (1997). Overexpressed IGF-I receptors reduce estrogen growth requirements, enhance survival, and promote E-cadherin-mediated cell-cell adhesion in human breast cancer cells. *Exp. Cell Res*. **231**, 149-162.

Guvakova, M. A. and Surmacz, E. (1999). The activated insulin-like growth factor I receptor induces depolarization in breast epithelial cells characterized by actin filament disassembly and tyrosine dephosphorylation of FAK, Cas, and paxillin. *Exp. Cell Res*. **251**, 244-255.

Guvakova, M. A., Boettiger, D. and Adams, J. C. (2002). Induction of fascin spikes in breast cancer cells by activation of the insulin-like growth factor-I receptor. *Int. J. Biochem. Cell. Biol*, **34**, 685-698.

Happerfield, L. C., Miles, D. W., Barnes, D. M., Thomsen, L. L., Smith, P. and Hanby, A. (1997). The localization of the insulin-like growth factor receptor 1 (IGFR-1) in benign and malignant breast tissue. *J. Pathology* **183**, 412-417.

Hay, E. D. (1995). An overview of epithelio-mesenchymal transformation. *Acta Anatomica* **154**, 8-20.

Hazan, R. B. and Norton, L. (1998). The epidermal growth factor receptor modulates the interaction of E-cadherin with the actin cytoskeleton. *J. Biol. Chem*. **273**, 9078-9084.

Hemmings, L., Kuhlman, P. A. and Critchley, D. (1992). Analysis of the actin-binding domain of α-actinin by mutagenesis and demonstration that dystrophin contains a functionally homologous domain. *J. Cell Biol.* **116**, 1369-1380.

Herrera, R. (1998). Modulation of hepatocyte growth factor-induced scattering of HT29 colon carcinoma cells. Involvement of the MAPK pathway. *J. Cell Sci.* **111**, 1039-1049.

Hijikata, T., Lin, Z. X., Holtzer, S., Choi, J., Sweeney, H. L. and Holtzer, H. (1997). Unanticipated temporal and spatial effects of sarcomeric α-actinin peptides expressed in PtK2 cells. *Cell Motil. Cytosleteton* **38**, 54-74.

Hu, Y., Qiao, L., Wang, S., Rong, S., Meuillet, E. J., Berggren, M., Gallegos, A., Powis, G. and Kozikowski, A. P. (2000). 3-(Hydroxymethyl)-bearing phophatidylinositol ether lipid analogous and carbonate surrogates block PI3-K, Akt, and cancer cell growth. *J. Med. Chem*. **43**, 3045-3051.

Isumi, T., Saeki, Y., Akanuma, Y., Takaku, F. and Kasuga, M. (1988). Requirement for receptor-intrinsic tyrosine kinase activities during ligand-induced membrane ruffling of KB cells. *J. Biol. Chem.* **263**, 10386-10393.

Izaguirre, G., Aguirre, L., Hu, Y. P., Lee, H. Y., Schlaepfer, D., Aneskievich, B. J. and Haimovich, B. (2001). The cytosleletal/non-muscle isoform of α-actinin is phosphorylated on its actin-binding domain by the focal adhesion kinase. *J. Biol. Chem.* **276**, 28676-28685.

Kadowaki, T., Koyasu, S., Nishida, E., Sakai, H., Takaku, F., Yahara, I. and Kasuga, M. (1986). Insulin-like growth factors, insulin, and epidermal growth factor cause rapid cytoskeletal reorganization in KB cells. *J. Biol. Chem.* **261**, 16141-16147.

Kato, H., Faria, T. N., Stannard, B., Roberts, C. T., Jr and LeRoith, D. (1994). Essential role of tyrosine residues 1131, 1135, 1136 of the insulin-like growth factor-I (IGF-I) receptor on IGF-I action. *Mol. Endocrinol.* **8**, 40-50.

Kleinberg, D. L., Feldman, M. and Ruan, W. (2000). IGF-I: an essential factor in terminal end bud formation and ductal morphogenesis. *J. Mamm. Gland Biol. Neoplasia* **5**, 7-17.

Klemke, R. L., Cai, S., Giannini, A. L., Gallagher, P. J., de Lanerolle, P. and Cheresh, D. A. (1997). Regulation of cell motility by mitogen-activated protein kinase. *J. Cell Biol.* **137**, 481-492.

Knudsen, K. A., Peralta Soler, A., Johnson, K. R. and Wheellock, M. J. (1995). Interactions of α-actinin with the cadherin/catenin cell-cell adhesion complex via α-catenin. *J. Cell. Sci*. **130**, 67-77.

Kohn, E. C., Francis, E. A., Liotta, L. A. and Schiffmann, E. (1990). Heterogeneity of the motility responses in malignant tumor cells: a biological basis for the diversity and homing of metastatic cells. *Int. J. Cancer* **46**, 287-292.

Kroemker, M., Rüdiger, A. H., Jockusch, B. M. and Rüdiger, M. (1994). Intramolecular interactions in vinculin control α-actinin binding to the vinculin head. *FEBS Lett*. **355**, 259-262.

Kureishy, N., Sapountzi, A., Prag, S., Anilkumar, N. and Adams, J. C. (2002). Fascins, and their roles in cell structure and function. *BioEssays* **24**, 350-361.

Kusumi, A., Suzuki, K. and Koyasako, K. (1999). Mobility and cytoskeletal interactions of cell adhesion receptors. *Curr. Opin. Cell. Biol.* **11**, 582-590.

Lee, A. V., Hilsenbeck, S. G. and Yee, D. (1998). IGF system components as prognostic markers in breast cancer. *Breast Cancer Res. Treat*. **47**, 295-302.

LeRoith, D. (2000). Insulin-like growth factor I receptor signaling-Overlapping or redundant pathways. *Endocrinol.* **141**, 1287-1288.

Leventhal, P. S. and Feldman, E. L. (1997). Insulin-like growth factors as regulators of cell motility: Signaling mechanisms. *Trends. Endocrinol. Metab.* **8**, 1-6.

Liang, T. J., Reid, A. E., Xavier, R., Cardiff, R. D. and Wang, T. C. (1996). Transgenic expressions of tpr-met oncogene leads to development of mammary hyperplasia and tumors. *J. Clin. Invest.* **97**, 2872-2877.

Manes, S., Mira, E., Gomes-Mouton, C., Zhao, Z. J., Lacalle, R. A. and Martinez-A, C. (1999). Concerted activity of tyrosine phosphatase SHP-2 and focal adhesion kinase in regulation of cell motility. *Mol. Cell. Biol.* **19**, 3125-3135.

Matsudaira, P. (1994). Actin crosslinking proteins at the leading edge. *Semin. Cell Biol.* **5**, 165-174.

McGregor, A., Blanchard, A. D., Rowe, A. J. and Critchley, D. R. (1994). Identification of the vinculin-binding site in the cytoskeletal protein alpha-actinin. *Biochem. J*. **301**, 225-233.

Mira, E., Manes, S., Lacalle, R. A., Marquez, G. and Martinez-A, C. (1999). Insulin-like growth factor I-triggered cell migration and invasion are mediated by matrix metalloproteinase-9. *Endocrinol.* **140**, 1657-1664.

Morali, O. G., Delmas, V., Moore, R., Jeanney, C., Thiery, J. P. and Larue, L. (2001). IGFII induces rapid β-catenin relocation to the nucleus during epithelium to mesenchyme transition. *Oncogene* **20**, 4942-4950.

Müller, T., Choidas, A., Reichmann, E. and Ullrich, A. (1999). Phosphorylation and free pool of β-catenin are regulated by tyrosine kinases and tyrosine phosphatases during epithelial cell migration. *J. Biol Chem.* **274**, 10173-10183.

Nieset, J. E., Redfield, A. R., Jin, F., Knudsen, K. A., Johnson, K. R. and Wheelock, M. J. (1997). Characterization of the interactions of alpha-catenin with alpha-actinin and beta-catenin/plakoglobin. *J. Cell Sci*. **110**, 1013-1022.

Nobes, C. D., Hawkins, P., Stephens, L. and Hall, A. (1995). Activation of

the small GTP-binding proteins rho and rac by growth factor receptors. *J. Cell Sci*. **108**, 225-233.

Otey, C. A., Vasquez, G. B., Burridge, K. and Erickson, B. W. (1993). Mapping of the α-actinin binding site with the β1 integrin cytoplasmic domain. *J. Biol. Chem.* **268**, 21193-21197.

Potempa, S. and Ridley, A. J. (1998). Activation of both MAP kinase and phosphatidylinositide 3-kinase by Ras is required for hepatocyte growth factor/scatter factor-induced adherens junction disassembly. *Mol. Biol. Cell* **9**, 2185-2200.

Resnik, J. L., Reichart, D. B., Huey, K., Webster, N. J. G. and Seely, B. L. (1998). Elevated insulin-like growth factor I receptor autophosphorylation and kinase activity in human breast cancer. *Cancer Res*. **58**, 1159-1164.

Royal, I. and Park, M. (1995). Hepatocyte growth factor-induced scatter of Madin-Darby Canine kidney cells requires phosphatidylinositol-3 kinase. *J. Biol. Chem*. **270**, 27780-27787.

Sachs, M., Weidner, K. M., Brinkmann, V., Walther, I., Obermeier, A., Ullrich, A. and Birchmeier, W. (1996). Motogenic and morphogenic activity of epithelial receptor tyrosine kinases. *J. Cell Biol*. **133**, 1095-1107.

Savagner, P. (2001). Leaving the neighborhood: molecular mechanisms involved during epithelial-mesenchymal transition. *BioEssays* **23**, 912-923.

Savagner, P., Yamada, K. M. and Thiery, J. P. (1997). The zinc-finger protein slug causes desmosome dissociation, an initial and necessary step for growth factor-induced epithelial-mesenchymal transition. *J. Cell Biol.* **137**, 1403-1419.

Schultheiss, T., Choi, J., Lin, Z. X., DiLullo, C., Cohen-Gould, L., Fischman, D. and Holtzer, H. (1992). A sarcomeric alpha-actinin truncated at the carboxyl end induced the breakdown of stress fibers in PtK2 cells and the formation of nemaline-like bodies and breakdown of myofibrils in myotubes. *Proc. Natl. Acad. Sci. USA* **89**, 9282-9286.

Shibasaki, F., Fukami, K., Fukui, Y. and Takenawa, T. (1994). Phosphatidylinositol 3-kinase binds to alpha-actinin through the p85 subunit. *Biochem. J.* **302**, 551-557.

Spencer, K. S. R., Graus-Porta, D., Leng, J., Hynes, N. E. and Klemke, R. L. (2000). ErbB2 is necessary for induction of carcinoma cell invasion by ErbB family receptor tyrosine kinases. *J. Cell Biol.* **148**, 385-397.

Stoker, M. and Perryman, M. (1985). An epithelial scatter factor released by embryo fibroblasts. *J. Cell Sci.* **77**, 209-223.

Stoker, M., Gherardi, E., Perryman, M. and Gray, J. (1987). Scatter factor is a fibroblast-derived modulator of epithelial cell mobility. *Nature* **327**, 239-242.

Thiery, J. P. and Chopin, D. (1999). Epithelial cell plasticity in development and tumor progression. *Cancer Metastasis Rev.* **18**, 31-42.

Tilney, L. G. and Tilney, M. S. (1994). Methods to visualize actin polymerization associated with bacterial invasion. *Methods Enzymol*. **236**, 476-481.

Tsarfaty, I., Resau, J. H., Rulong, S., Keydar, I., Faletto, D. L. and Vande Woude, G. F. (1992). The met proto-oncogene receptor and lumen formation. *Science* **257**, 1258-1261.

Tseng, Y., Fedorov, E., McCaffery, J. M., Almo, S. and Wirtz, D. (2001). Micromechanics and ultrastructure of actin filament networks crosslinked by human fascin: a comparison with α-actinin. *J. Mol. Biol*. **310**, 351-366.

Tsukatani, Y., Sizuki, I. and Takahashi, K. (1997). Loss of density-dependent growth inhibition and dissociation of alpha-catenin from E-cadherin. *J. Cell. Physiol*. **173**, 54-63.

Vasioukhin, V., Bauer, C., Yin, M. and Fuchs, E. (2000). Directed actin polymerization is the driving force for epithelial cell-cell adhesion. *Cell* **100**, 209-219.

Weidner, K. M., Behrens, J., Vanderkerckhove, J. and Birchmeier, W. (1990). Scatter Factor: Molecular characteristics and effect on the invasiveness of epithelial cells. *J. Cell Biol*. **111**, 2097-2108.

Witke, W., Hofmann, A., Koppel, B., Schleicher, M. and Noegel, A. A. (1993). The Ca^{2+}-binding domains in non-muscle type alpha-actinin: biochemical and genetic analysis. *J. Cell Biol*. **121**, 599-606.

Wong, V., Ching, D., McCrea, P. D. and Firestone, G. L. (1999). Glucocorticoid down-regulation of fascin protein expressions is required for the steroid-induced formation of tight junctions and cell-cell interactions in rat mammary epithelial tumor cells. *J. Biol. Chem.* **274**, 5443-5453.

Xu, J., Wirtz, D. and Pollard, T. D. (1998). Dynamic cross-linking by α-actinin determines the mechanical properties of actin filament networks. *J. Biol. Chem.* **273**, 9570-9576.

Yamashiro, S., Yamakita, Y., Ono, S. and Matsumura, F. (1998). Fascin, an actin-bundling protein, induces membrane protusions and increases cell motility of epithelial cells. *Mol. Biol. Cell* **9**, 993-1006.